THE ASTROPHYSICAL JOURNAL, **239**:12–37, 1980 July 1

A DISTANCE SCALE FROM THE INFRARED MAGNITUDE/H I VELOCITY-WIDTH RELATION. III. THE EXPANSION RATE OUTSIDE THE LOCAL SUPERCLUSTER

MARC AARONSON[1]
Steward Observatory, University of Arizona

JEREMY MOULD
Mount Wilson and Las Campanas Observatories, Carnegie Institutiion of Washington; and Kitt Peak National Observatory[2]

JOHN HUCHRA[1]
Harvard-Smithsonian Center for Astrophysics

AND

WOODRUFF T. SULLIVAN III,[3] ROBERT A. SCHOMMER,[3] AND GREGORY D. BOTHUN[3]
Department of Astronomy, University of Washington, Seattle
Received 1979 December 5; accepted 1980 January 11

ABSTRACT

Infrared magnitudes and 21 cm H I velocity widths are presented for galaxies in the Pegasus I cluster ($V \approx 4000$ km s^{-1}), the Cancer cluster ($V \approx 4500$ km s^{-1}), cluster Zwicky 1400.4+0949 (Z74-23) ($V \approx 6000$ km s^{-1}), and the Perseus supercluster ($V \approx 5500$ km s^{-1}). The data are used to determine redshift-independent distances from which values of the Hubble ratio can be derived. With a zero point based solely on the Sandage-Tammann distances to M31 and M33, the following results are obtained (zero-point error excluded):

Pegasus I.—$r = 42 \pm 4$ Mpc, $V/r = 91 \pm 8$ km s^{-1} Mpc^{-1};
Cancer.—$r = 49 \pm 6$ Mpc, $V/r = 89 \pm 11$ km s^{-1} Mpc^{-1};
Z74-23.—$r = 61 \pm 4$ Mpc, $V/r = 96 \pm 7$ km s^{-1} Mpc^{-1};
Perseus supercluster.—$r = 53 \pm 2$ Mpc, $V/r = 104 \pm 6$ km s^{-1} Mpc^{-1}.

The closely similar value of the Hubble ratio found in the four independent samples suggests that the zero-point calibration in the IR/H I technique does not depend on environment. The difference between the mean of these Hubble ratios, $V/r = 95 \pm 4$ km s^{-1} Mpc^{-1}, and that measured for Virgo in Paper II, $V/r = 65 \pm 4$ km s^{-1} Mpc^{-1}, is significant at a formal level of 5 σ.

The simplest explanation of the discrepancy is to postulate a Local Group component of motion in the direction of Virgo. The resulting velocity perturbation is $\Delta V = 480 \pm 75$ km s^{-1}. This value agrees well with recent observations of a dipole term in the 3 K microwave background, the only other anisotropy test for which a detection significance of 5 σ or more is claimed. We are thus led to a preliminary estimate for the value of the Hubble constant of $H_0 = 95 \pm 4$ km s^{-1} Mpc^{-1}. If a zero point based on de Vaucouleurs's distances to M31 and M33 is adopted instead, all distances *decrease* by 18%, and the Hubble constant *increases* by a similar amount.

A variety of possible systematic errors which might affect the present conclusions are investigated, but we can find none that are relevant. In particular, because the galaxy samples are chosen from a cluster population which is generally all at the same distance, Malmquist bias does not occur. In fact, two of the clusters (Pegasus I and Z74-23) are sampled in both magnitude and velocity width to a level as deep as Virgo itself.

Other observational data related to the value of H_0 are examined, as are a number of previously used anisotropy tests, including color-luminosity relations, brightest cluster member(s), central surface brightnesses, and supernovae. We find that some of these tests support the present results, while contrary evidence is currently weak.

[1] Guest Investigator at Kitt Peak National Observatory.

[2] Operated by the Association of Universities for Research in Astronomy, Inc., under contract with the National Science Foundation.

[3] Guest Investigator at Arecibo Observatory, which is part of the National Astronomy and Ionospheric Center, operated by Cornell University, under contract with the National Science Foundation.

A model in which Virgo gravitationally retards the Hubble flow of galaxies within the Local Supercluster provides a natural interpretation of our findings. A range of 1.5–3 in local density contrast then leads to a value of the density parameter $\Omega \approx 0.7$–0.2. The deceleration parameter q_0 is then 0.35–0.1 for a simple Friedmann-type expanding universe.

Subject headings: cosmology — galaxies: clusters of — galaxies: photometry — radio sources: 21 cm radiation

I. INTRODUCTION

The determination of the Hubble expansion rate H_0 has been complicated by the continuing controversy over perturbations in the local kinematic field. For instance, Rubin *et al.* (1976) find a velocity component of some 600 km s^{-1} in a direction nearly perpendicular to the Virgo cluster, while the results of two independent 3 K microwave-background experiments (Cheng *et al.* 1979; Smoot, Gorenstein, and Muller 1977) indicate a component of comparable size but in a direction more nearly toward Virgo. On the other hand, Sandage and Tammann (1975*a*, *b*) find no evidence at all for anisotropic motions. To resolve this matter, it is clearly essential to measure accurate redshift-independent distances to galaxies that have recession velocities exceeding 3000 km s^{-1}.

A number of techniques are available for bridging the gap between distances within the Local Group (which themselves require further attention) and distances beyond the Local Supercluster. Among these yardsticks for the universe are the calibration of luminosity classes in terms of magnitudes and/or diameters (e.g., Sandage and Tammann 1975*a*, *b*; de Vaucouleurs and Bollinger 1979) and the study of supernovae (Tammann 1978). The most recent addition to this distance-measuring equipment is the 21 cm profile method pioneered by Tully and Fisher (1977). Technological advances in the form of increased size and sensitivity of radio telescopes now enable this method to reach redshifts greater than 10,000 km s^{-1}. In addition, the use of infrared rather than optical magnitudes greatly reduces the various uncertainties inherent in its practical application (Aaronson, Huchra, and Mould 1979, hereafter AHM).

This is the third paper in a series devoted to measurement of the distance scale, using the infrared magnitude/H I velocity-width relation. In Paper I (Aaronson, Mould, and Huchra 1980) we derived distances to nearby groups which were shown to agree well with the relative scale constructed by Sandage and Tammann. In Paper II (Mould, Aaronson, and Huchra 1980) we determined a distance to the Virgo cluster which led to a Hubble ratio of 65 ± 4 km s^{-1} Mpc^{-1}. The dependence of this result on morphological type, magnitude and radio flux limits, and inclination (for $i > 45°$) was also investigated and found to be unimportant.

In the present paper we turn our attention to four nearby clusters in the redshift range 4000–6000 km s^{-1} distributed across the sky. We emphasize that the study of clusters effectively combats the Malmquist bias, since the cluster galaxies are all at similar distances. At the same time, an additional uncertainty is introduced. Is the luminosity/velocity-width relation dependent in some way on cluster environment? To answer this question, we have chosen a sample containing different cluster types (§ II). In §§ III–V we gather and discuss the data required to construct the various infrared Tully-Fisher diagrams. The resulting distance moduli and Hubble ratios give considerable support for anisotropic motion in the direction of Virgo (§ VI). Possible sources of systematic error are discussed in § VII, including the question of intrinsic cluster differences, which we suggest are unlikely to be significant. Finally, a critical examination of other distance estimators in § VIII reveals that there are no overriding inconsistencies with the present results. The principal conclusions of this paper include a preliminary estimate for the value of $H_0 = 95 \pm 4$ km s^{-1} Mpc^{-1} and a strong indication of the kinematic influence of the Virgo mass concentration; several cosmological implications of these results are discussed in § IX.

II. THE CLUSTER SAMPLE

Some properties of the clusters studied here are summarized in Table 1. Pegasus I and Cancer are discussed in the pioneering paper of Humason, Mayall, and Sandage (1956), while Zwicky 1400.4 +0949 is a medium-compact cluster from the catalog of Zwicky *et al.* (1961–1968). (For the sake of brevity, we refer to the latter cluster as Z74-23.)

All three clusters are sparse (Abell richness class 0) and spiral rich. The cluster radii (col. [3]) are based on contours drawn by Zwicky *et al.* (1961–1968) which we adopt here as delineating the nominal cluster boundaries. Also given in Table 1 are the ratios of ellipticals to spirals following Nilson (1973, hereafter UGC), Sandage's population index (N_c^{48}), and the Bautz-Morgan (B-M) concentration class. For further comparison, N_c^{48} and B-M type for Virgo are 60 and III, respectively (Sandage and Hardy 1973). Recent discussions of these clusters are given by Chincarini and Rood (1976); Tifft, Jewsbury, and Sargent (1973); and Thompson, Welker, and Gregory (1978).

The fourth "cluster" in Table 1 is a sample taken from the Perseus supercluster. According to Jôeveer, Einasto, and Tago (1978), the Perseus supercluster encompasses a long chain of cluster cores (including Abell 262 and the Pisces and Perseus clusters) forming the supercluster boundary along the north, plus a diffuse region of galaxies stretching south to Abell 194. The full extent of the supercluster is some 70° across

TABLE 1

CLUSTER PROPERTIES

Name	Position[a] RA ℓ	Position[a] Dec b	Angular Size Radius/h[b] (Mpc)	N_C[48] E/Sp[c]	Types Abell B-M
Pegasus I........	$23^h17^m.7$	07° 55'	6°.3	59	0
UGC 487..........	88°	−48°	2.1	0.1	II
Cancer...........	$08^h17^m.7$	21° 14'	4.0	17	0
UGC 118..........	203°	29°	1.6	0.1	III
Zwicky 74-23.....	$13^h59^m.7$	09° 41'	2.2	30	0
UGC 313..........	350°	66°	1.2	0.1	---
Perseus..........	$23^h \rightarrow 4^h$	−5° → 45°	70°	---	---
Supercluster	---	---	---	---	---

[a]Positions given are NGC 7619 (for Pegasus I), NGC 2563 (for Cancer), and NGC 5416 (for Z74-23). Extent of Perseus Supercluster is adopted from Jôeveer, Einasto, and Tago (1978).

[b]$h = H_0/100$.

[c]E/Sp = the ratio of the number of ellipticals to spirals as classified by Nilson (1973).

TABLE 2

21 cm VELOCITY WIDTHS

Name	i[a] (deg)	ΔV_{50} (km s^{-1})	σ_{50} (km s^{-1})	ΔV_{20} (km s^{-1})	σ_{20} (km s^{-1})	S/N	Source[b]
			Pegasus I				
UGC 12417......	66	262	+12−20	285	+27−12	5	1
UGC 12423......	90	501	±6	535	+17−12	13	1
UGC 12442......	81	315	±15	353	±20	10	1
		302	±27	352	---	7	4
				353 adopted			
UGC 12447......	74	430	+10−7	477	±8	15	1
		---	---	472	---	12	3
		430	+17	461	---	10	4
				473 adopted			
UGC 12486......	68	383	+12−9	436	+25−11	9	1
UGC 12494......	74	212	±7	253	+13−28	8	1
UGC 12497......	83	169	+21−26	209[c]	---	4	1
UGC 12498......	72	265	+38−18	299[c]	---	3	1
UGC 12539......	66	365	+8−7	381	±8	4	1
Z406-086.......	84	194	+21−60	221	+24−20	3	1
			Cancer				
UGC 4329......	55	220	±21	248	−12+66	4	1
Z119-053......	50	195	+16−23	226	+19−24	4	1
UGC 4334......	70	403	+15−10	439	+22−15	8	1
UGC 4354......	60	294	+12−18	314	+13−64	3	1
UGC 4386......	80	485[d]	±10	516[c]	---	5	1
UGC 4399......	72	221	+10−15	271	+10−21	5	1
			Zwicky 74-23				
UGC 8918.......	89	316	+14−16	339	+22−15	4	7
		---	---	338	---	7	2
				339 adopted			
UGC 8938.......	52	341	±8	363	+16−12	6	7
		---	---	361	---	7	2
				362 adopted			
UGC 8942.......	48	---	---	322	---	5	2
UGC 8944.......	60	322	±11	347	+19−15	4	7
		---	---	361	---	7	2
				354 adopted			
UGC 8948.......	65	321	+29−16	368	+16−25	4	7
		---	---	378	---	7	2
				373 adopted			
UGC 8950.......	90	---	---	206	---	5	2
UGC 8951.......	88	---	---	266	---	4	2
UGC 8967.......	90	370	+16−19	392	+26−15	8	7
		---	---	383	---	6	2
				388 adopted			
UGC 9023.......	68	---	---	268	---	4	2

TABLE 2—*Continued*

Name	Type	V (km s^{-1})	V_0 (km s^{-1})	i[a] (deg)	ΔV_{50} (km s^{-1})	σ_{50} (km s^{-1})	ΔV_{20} (km s^{-1})	σ_{20} (km s^{-1})	S/N	Source[b]
					Perseus Supercluster					
UGC 94........	Sb	4602	4827	48	309	±5	331	+27-8	7	5
UGC 98........	SBb	4796	5037	62	322	+4-81	333	+23-12	6	5
UGC 100.......	Sb-c	4797	5039	65[e]	387	±5	403	±4	6	5
UGC 238.......	S	6785	7015	81	396	+8-34	435	±28	5	5
UGC 255.......	S	6281	6511	65	363	+8-9	397[c]	---	3	5
UGC 279.......	SB?	6276	6503	76	431	+11-21	456	+9-11	5	5
UGC 433.......	Sc	4656	4878	90	---	---	442	±20	5	5
UGC 562.......	SBb	5456	5669	69	455	+14-27	478	+25-4	5	5
UGC 927.......	Sb-c	5997	6197	61	294	+18-33	326[c]	---	3	5
UGC 979.......	Pec	4796	4995	81	---	---	528:	---	5	6
UGC 1577......	SBb	5277	5442	46:	275	±3	303	+39-10	9	5
UGC 1835......	Sc	5082	5225	57[f]	346	±7	372	+13-9	6	5
UGC 2134......	Sb	4565	4695	66	332	±5	359	+11-9	9	5
UGC 2274......	S	5257	5401	53	365	±10	386	+50-13	5	5
UGC 12666.....	Sc	4984	5241	65	294	+11-20	320	+6-8	7	5

[a] i is from Danver (1942) for UGC 12442 and 12447; otherwise it is calculated from equation (4) of Paper I, using axial ratios in the RC2 or transformed to that system.

[b] Sources for velocity widths are (1) Schommer, Sullivan, and Bothun (1980), data for UGC 4399 will be published separately; (2) Chincarini, Giovanelli, and Haynes (1980); (3) Shostak (1978); (4) Krumm and Salpeter (1979); (5) Bania, Thompson, and Thuan (1980) recalibrated as in Sullivan *et al.* (1980); (6) Bania, Thompson, and Thuan (1980); (7) Sullivan *et al.* (1980).

[c] ΔV_{20} is found by extrapolation of ΔV_{50}, using Fig. 1.

[d] Interference spike on the edge of profile; ΔV_{50} could be as much as 20 km s^{-1} larger.

[e] Danver's (1942) value of $i = 50°$ has been ignored.

[f] Inner arm structure suggests low inclination; the 3° correction was not applied to axial ratio formula (Paper I).

the sky. Our sample is drawn chiefly from the northern intercluster region and represents a set of galaxies from a low-density environment more comparable to that of nearby field galaxies. Since the velocity dispersion is low and the mean redshift remains constant along the supercluster chain (Gregory, Thompson, and Tifft 1980), all the galaxies may be regarded as lying roughly at the same distance.

III. H I VELOCITY WIDTHS

H I velocity widths for galaxies in the present sample are presented in Table 2. The observing and reduction procedures are fully described in the sources quoted in column (8); the 21 cm profiles are also given in these sources. With one exception, the observations in Table 2 were obtained with the Arecibo 305 m telescope.

The sample of galaxies observed at 21 cm by Sullivan *et al.* (1980) and by Schommer, Sullivan, and Bothun (1980) (the primary data sources) were originally chosen for the purpose of studying the H I properties of cluster spirals. The selection criteria were (in order of importance) that the galaxy (1) be considered a cluster member, (2) be bright and classified as a spiral, (3) have a measured redshift, and (4) be listed in the UGC. Similar criteria were employed by Bania, Thompson, and Thuan (1980), who, in their study of the Perseus supercluster, also applied a strict limit of $m_{pg} < 15$ (using magnitudes from Zwicky *et al.* 1961–1968). The original calibrated profiles from Bania, Thompson, and Thuan (1980) were kindly made available to us for this work and were then treated in an identical manner to those from Sullivan *et al.* (1980).

In selecting the present sample, three further criteria were employed. First, the galaxy inclination was required to be $> 45°$ (see Paper I). Second, only profiles with a signal-to-noise (S/N) level (as defined below) $\gtrsim 3$ and having steeply sloping sides were accepted. Third, only galaxies sufficiently isolated to avoid confusion problems were chosen.

The galaxies in Table 2 are identified by either their UGC or Zwicky *et al.* (1961–1968) designations (col. [1]), and our adopted inclinations to the plane of the sky are also given (col. [2]), based largely on UGC axial ratios (footnote *a*). The line widths in columns (3) and (5) are listed for the 50% (when available) and 20% levels, respectively, following the definitions of Paper I. These have not been corrected for instrumental resolution or internal galaxy turbulence. The errors listed in columns (4) and (6) were obtained in the following fashion. The definition of "edge" point in each case was allowed to vary by $\pm \Delta S_{rms}$ (the rms noise in the profile, estimated from the baseline), and the resultant line widths were recalculated. The errors estimated in this way are often asymmetric, dependent upon the shape and S/N in each profile (see Sullivan *et al.* 1980 for further details). Column (7) gives the value

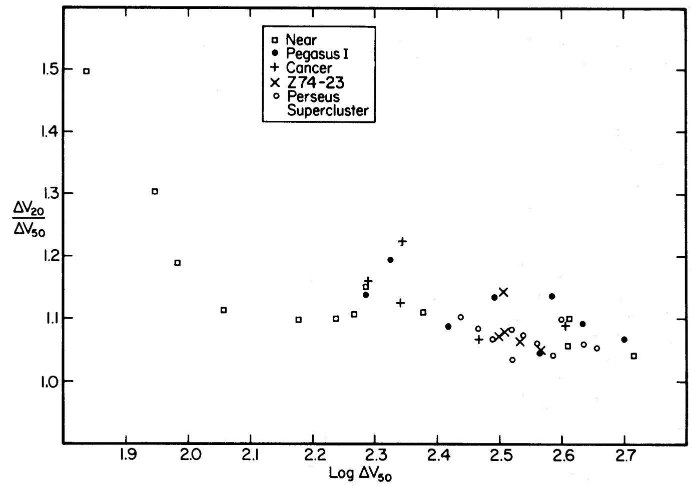

FIG. 1.—The ratio of observed H I velocity width at the 20% level to that at the 50% level vs. log velocity width at the 50% level for all of the nearby galaxies in Paper I and this paper.

of S/N, defined as the ratio of the estimated mean signal (over the *entire* extent of the profile) to $\Delta S_{\rm rms}$.

Note that the last part of Table 2 (Perseus supercluster) differs slightly in format in that the morphological type (from the UGC), heliocentric H I velocity, and velocity corrected for solar motion (as in § V) are given in columns (2), (3), and (4), respectively.

In Figure 1 we have plotted the ratio $\Delta V_{20}/\Delta V_{50}$ against log ΔV_{50} for all the galaxies in Paper I and in this paper. The expected trend with log ΔV_0 is apparent (see Paper I). We have used Figure 1 to extrapolate the value of ΔV_{50} to ΔV_{20} in five cases of low S/N (Table 2). Based on Figure 1, we estimate that for log $\Delta V_{50} > 2.2$, ΔV_{20} can be so obtained with an additional error of only $\sim 5\%$.

Owing to the proximity of NGC 7537 and 7541 (separation 3′) in Pegasus I and their almost identical velocities (§ V), there is some danger that the H I signals are confused. Three arguments suggest this is not the case. First, the 21 cm profiles of both galaxies exhibit no asymmetries and thus appear distinct. Second, the sum of the measured H I flux density for the two galaxy positions obtained by Schommer, Sullivan, and Bothun (1980) agrees well with the flux measured by Shostak (1978), whose 10′ beam included both objects. Finally, the Krumm and Salpeter (1979) Arecibo velocity widths agree well with those of Sullivan *et al.* (1980). Had there been significant confusion, such good agreement would not have been expected in view of the pointing uncertainty ($\sim 0\rlap{.}'5$) in the 305 m dish.

The observed values of ΔV_{20} have been corrected both for inclination and for the relativistic Doppler effect $(1 + z)$ according to

$$\Delta V_{20}{}^{c}(0) = \frac{\Delta V_{20}}{\sin i(1 + z)} \cdot \qquad (1)$$

(The final velocity widths are recorded in col. [4] of Table 6.)

IV. INFRARED OBSERVATIONS

a) Observed Magnitudes

Magnitudes at H (1.6 μm) have been measured for all the galaxies with velocity widths discussed in § III. The Harvard-Smithsonian InSb detector system was used at the Kitt Peak National Observatory 2.1 m and Steward Observatory 2.25 m telescopes. In addition, some data were obtained with the KPNO Otto system on the 1.3 m telescope and also with Caltech IR photometer No. 1 at Mount Wilson and Palomar. With the exception of the Otto system, where a TV guider was used to view the object through a dichroic filter, acquisition was always accomplished by using precision ($\sim 1''$) offsets premeasured with the KPNO Grant measuring engine.[4] Correct centering was then verified by perpendicular scans through the galaxy. Only rarely did this necessitate small additional offsets. When a field star or extended flux from the galaxy occurred in the reference beam, either the photometer was rotated from nominal north-south alignment or the measurement was made "single beam."

Correction of the photometry for instrumental effects and reduction to the standard system follow the procedures fully described in Paper I. Isophotal diameters for the program objects corrected to the system of Paper I are given in column (2) of Table 3. The final H magnitude and corresponding aperture sizes A are recorded in columns (3) and (4). The isophotal diameters essentially correspond to the system of de Vaucouleurs, de Vaucouleurs, and Corwin (1976, hereafter RC2), differing only in regard to the galactic extinction correction and a cutoff term applied to highly inclined objects (see Paper I). Diameters from the RC2 are actually available for only a few galaxies in Table 3. For most of the remaining objects, we

[4] Accurate positions for all the objects in Table 2 and for a large number (~ 500) of additional galaxies in these and other clusters and in the field are available from the authors.

TABLE 3

INFRARED MAGNITUDES OF GALAXIES

Name	log D_1 [a]	H (mag)	A (arcsec)	log A/D_1	Tel
		Pegasus I			
UGC 12417......	1.00	11.64	23.7	-0.40	KP 50
IC 1474		11.26	33.8	-0.25	"
UGC 12423......	1.39	11.19±0.04	33.8	-0.64	"
		10.86	47.7	-0.49	"
UGC 12442......	1.25	10.97	23.7	-0.65	"
NGC 7537		10.78	33.8	-0.50	"
		10.60	47.7	-0.35	"
UGC 12447......	1.44	10.20	23.7	-0.84	KP 84
NGC 7541		9.59	36.2	-0.66	"
		9.38	46.8	-0.55	"
		9.26	48.7	-0.53	"
		8.93	72.5	-0.36	"
UGC 12486......	1.21	10.55	23.7	-0.61	"
NGC 7591		10.36	33.8	-0.46	KP 50
		10.29	36.2	-0.43	KP 84
		10.21	47.7	-0.31	KP 50
UGC 12494......	1.09	13.43±0.05	23.7	-0.49	KP 84
UGC 12497......	0.93	13.44±0.06	23.7	-0.33	"
		13.03±0.05	36.2	-0.15	"
UGC 12498......	1.10	11.91±0.04	17.5	-0.64	"
IC 5309		11.71	22.5	-0.53	"
UGC 12539......	1.22	11.01	23.7	-0.62	KP 50
NGC 7631		10.98	23.7	-0.62	KP 84
		10.68	33.8	-0.47	KP 50
		10.61	36.2	-0.44	KP 84
Z406-086	0.87	13.21±0.08	17.5	-0.40	"
		Cancer			
UGC 4329.......	1.36	12.62±0.04	17.2	-0.90	SO 90
		12.18±0.04	23.1	-0.77	KP 84
		12.00	27.0	-0.71	SO 90
		11.70	36.2	-0.58	KP 84
		11.70	36.7	-0.57	SO 90
		11.46	46.8	-0.47	KP 84
Z119-053.......	0.80	13.16	9.75	-0.59	P 200
		12.91	13.25	-0.46	"
		12.88±0.05	17.5	-0.34	KP 84
		12.49±0.06	23.1	-0.21	"
UGC 4334.......	1.21	10.36	17.2	-0.75	SO 90
NGC 2565		10.04	27.0	-0.56	"
		9.68	36.7	-0.42	"
UGC 4354.......	1.09	12.70±0.04	13.5	-0.74	"
NGC 2570		12.51	17.2	-0.63	"
		12.19	27.0	-0.44	"
UGC 4386.......	1.17	11.04	17.2	-0.71	"
		10.70	27.0	-0.52	"
		10.52	36.7	-0.38	"
UGC 4399.......	0.97	13.06	17.5	-0.51	KP 84
		12.80	22.8	-0.39	"
		12.81±0.08	24.0	-0.37	MW 60
		Zwicky 74-23			
UGC 8918.......	1.09	11.80	23.1	-0.51	KP 84
		11.57	36.2	-0.31	"
UGC 8938.......	1.20	11.42	23.1	-0.61	"
NGC 5409		11.19	36.2	-0.42	"
UGC 8942.......	1.00	11.75	17.5	-0.53	"
NGC 5414		11.60	22.5	-0.42	"
UGC 8944.......	1.13	11.31	23.1	-0.54	"
NGC 5416		10.87	36.2	-0.35	"
UGC 8948.......	1.12	11.94	23.1	-0.53	"
		11.70	36.2	-0.34	"
UGC 8950.......	0.95	15.11[b] ± 0.06	13.3	-0.60	P 200
		14.44 ± 0.09	17.5	-0.49	KP 84
		14.30 ± 0.13	23.1	-0.36	"
UGC 8951.......	0.92	13.85 ± 0.07	17.5	-0.46	"
		13.63 ± 0.05	23.1	-0.33	"
UGC 8967.......	1.11	11.75	23.1	-0.52	"
		11.48	36.2	-0.33	"
UGC 9023.......	1.02	14.03 ± 0.05	17.5	-0.56	"
		13.71 ± 0.04	22.5	-0.45	"

TABLE 3—*Continued*

Name	log D_1 [a]	H (mag)	A (arcsec)	log A/D_1	Tel
		Perseus Supercluster			
UGC 94.........	1.32	11.68 ± 0.06	23.1	-0.73	KP 84
NGC 26		11.11 ± 0.04	36.2	-0.54	"
UGC 98.........	1.09	11.59	17.5	-0.63	"
NGC 21		11.35	23.1	-0.50	"
		10.99	36.2	-0.31	"
UGC 100........	1.19	11.27	23.7	-0.59	"
NGC 29		10.87	36.2	-0.41	"
UGC 238........	1.19	11.44	23.7	-0.59	"
		11.09	36.2	-0.41	"
UGC 255........	1.07	11.54	17.5	-0.61	"
NGC 112		11.39	23.1	-0.48	"
UGC 279........	1.18	11.48	23.1	-0.59	"
		11.13	36.2	-0.40	"
UGC 433........	1.14	11.39	23.7	-0.54	"
		11.08	36.2	-0.36	"
UGC 562........	1.27	10.27	27.0	-0.62	SO 90
NGC 295		10.09	36.2	-0.49	KP 84
		10.08	36.7	-0.48	SO 90
		9.87	46.8	-0.38	KP 84
UGC 927........	1.19	12.06	23.7	-0.59	"
NGC 496		11.51	36.7	-0.41	"
UGC 979[c].......	1.38	10.62	36.2	-0.60	"
NGC 523		10.31	46.8	-0.49	"
UGC 1577.......	1.36	10.90	36.2	-0.58	"
		10.65	46.8	-0.47	"
UGC 1835.......	1.30	10.85	36.2	-0.52	"
IC 221		10.63	46.8	-0.41	"
UGC 2134.......	1.20	11.19	23.7	-0.60	"
		10.77	36.2	-0.42	"
UGC 2274.......	1.32	10.86	36.2	-0.54	"
NGC 1093		10.75	46.8	-0.43	"
UGC 12666......	1.13	12.48 ± 0.04	23.7	-0.53	"
		11.89	36.2	-0.35	"

[a]Diameters for two galaxies, Z406-086 and Z119-053, were measured off POSS plates by M.A. and then treated like UGC sizes. Otherwise, diameters are from the RC2 or the UGC (transformed to the RC2 system). D_1 is in units of 0'.1.

[b]Centering may be off.

[c]Aperture was centered on the brightest spot, which lay on the edge of this peculiar galaxy.

transformed measurements in the UGC to the RC2 system, using the formulae given in the latter reference. For two objects not listed in the UGC, one of us (M. A.) measured the images on glass copies of the Palomar Observatory Sky Survey; the results were transformed to the RC2 system precisely like UGC diameters. Sizes for a number of galaxies also measured as a control agreed very well with those listed in the UGC. Further discussion of the diameter system employed in this series of papers can be found in § VII.

b) *Corrected Magnitudes*

As in Papers I and II, we have determined for each galaxy the H magnitude at log $A/D_1 = -0.5$, referred to as $H_{-0.5}$ (col. [2] of Table 6). Two corrections are applied to the observed $H_{-0.5}$ values. First, we correct for galactic extinction according to a simple cosecant law, i.e., $A_H = 0.015[\csc(b) - 1]$ (Paper I). Second, we correct the H magnitudes for the effects of cosmological expansion on the measured (blue) isophotal diameters. As compared with a galaxy at rest, the diameter (and thus magnitude) of a galaxy at redshift z will be underestimated, owing to the change in surface brightness by $(1 + z)^4$ (Sandage 1961) and by k-dimming. To derive the size of this effect, we start with Freeman's (1970) surface brightness distribution for an exponential disk,

$$I(r) = I_0 e^{-\alpha r} , \tag{2}$$

where r is the radius, α is the scale length, I_0 is the central surface brightness, and I is the surface brightness at which r (or the diameter) is measured. Taking I_D to be the diminished central surface brightness, we have for low redshift

$$I_D \approx \frac{I_0}{(1+z)^4(1+k[z])} \approx \frac{I_0}{1+4z+2z} , \tag{3}$$

where $k(z) \approx 2z$ mag is adopted from Pence (1976). From equation (2),

$$\frac{\Delta r}{r} = \frac{\ln I_0/I - \ln I_D/I}{\ln I_0/I} = \frac{\ln I_0/I_D}{\ln I_0/I} . \tag{4}$$

With $I_0 = 21.65$ mag arcsec^{-2} (Freeman 1970) and $I = 25$ mag arcsec^{-2}, we then have

$$\frac{\Delta r}{r} \approx \frac{\ln(1+6z)}{\ln(21.9)} \approx \frac{6z}{3.085}, \quad (5)$$

and

$$\Delta \log D = \log\left(1 + \frac{\Delta r}{r}\right) \approx 0.8z\,. \quad (6)$$

Taking a value of 2.4 for the slope of the H growth curve at $\log A/D = -0.5$ (see AHM), we finally obtain a magnitude correction term given by $1.9z$, an approximation accurate for $z \lesssim 0.04$. Note that the size of the correction is rather small, being only 0.04 mag at $V = 6000$ km s^{-1}. Our fully corrected H magnitudes (col. [3] of Table 6) are thus obtained from the observed values according to

$$H^c = H - 0.015[\csc(b) - 1] - 1.9z\,. \quad (7)$$

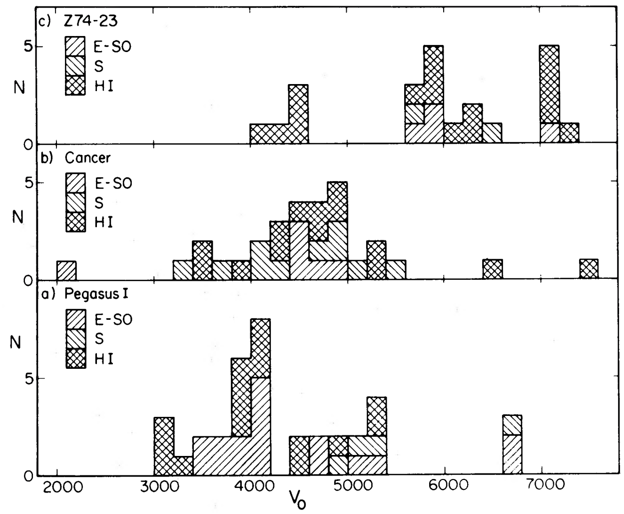

FIG. 2.—Redshift histograms for the data in Table 4. Hubble types and redshift sources are indicated.

V. MEAN REDSHIFTS AND CLUSTER MEMBERSHIP

A survey of the literature for redshifts in the Pegasus I, Cancer, and Z74-23 clusters yielded the results given in Table 4. Unless otherwise noted, the morphological types (col. [3]) are taken from the UGC or RC2, and the magnitudes (col. [4]) are from Zwicky *et al.* (1961–1968). The errors given in column (6) for the optical redshifts (col. [5]) are in a nominal sense only and are based on a combination of published errors and our own judgment. When both optical and H I (col. [8]) velocities exist for the same object, the adopted redshift is generally that given from H I. Our justification for this is, first, the radio redshifts are of much higher accuracy, and, second, the mean difference $\langle V_{\rm radio} - V_{\rm optical}\rangle$ is very small (see below). The final redshifts (col. [10]) are corrected for solar motion according to $V_0 = V + 300 \sin l^{\rm II} \cos b^{\rm II}$. The data for each cluster are discussed below.

Pegasus I.—In compiling redshifts, a low-velocity cutoff of 1000 km s^{-1} was used to exclude foreground objects, and a high-velocity cutoff of 7000 km s^{-1} was employed to exclude members of the Pegasus II cluster and other obvious background objects. Redshifts for 37 galaxies are then available, a histogram of which is shown in Figure 2*a*.

Three galaxies (Z406-009, UGC 12407, and UGC 12472) appear to be clearly background. Mean redshifts for various combinations of the remaining objects are given in Table 5. Several arguments suggest that the low-redshift pair NGC 7537 and 7541 are doubtful cluster members. First, the three brightest galaxies in the cluster are NGC 7541 ($B_T = 12.45$ mag in the RC2) and the two giant ellipticals NGC 7619 ($B_T = 12.1$ mag) and NGC 7626 ($B_T = 12.25$ mag). However, even a conservative correction for internal absorption would make the spiral NGC 7537 the brightest cluster member, a perhaps unusual situation for a cluster of B-M class II. For comparison, consider Virgo (B-M class III), whose brightest member NGC 4472 ($B_T = 9.31$ mag) is much brighter than the brightest Virgo spirals.[5] Second, the four largest spirals in Pegasus I listed in the UGC are UGC 12423 ($d = 3'.6$), NGC 7541 ($d = 3'.4$), NGC 7610 ($d = 2'.7$), and NGC 7537 ($d = 2'.1$), i.e., each of the pair is among the biggest galaxies in the region. Perhaps most significantly, the pair is located on the southernmost edge of the cluster contour drawn by Zwicky (1961–1968), far from the cluster center. However, by analogy with Virgo (Sandage and Tammann 1976*a*), we expect objects on the low-velocity tail to be near the cluster core for potential energy reasons. In fact, the next two lowest-redshift objects (UGC 12522 and 12544) are indeed close to the cluster core. In view of these arguments, we consider the best value for mean cluster redshift to be $V_0 = 3983 \pm 90$ km s^{-1} (Table 5. Here, as elsewhere, the luminosity-weighted mean is preferred. since we are interested in the dynamical cluster center. Finally, we note that the mean difference $\langle V_{\rm optical} - V_{\rm HI}\rangle = -3 \pm 21$ km s^{-1} for 13 galaxies.

Cancer.—Redshifts for 30 objects are available and are listed in Table 4*b*; the velocity distribution is also shown in Figure 2*b*. NGC 4367 and 4409 appear to be obvious foreground and background galaxies, respectively. Mean redshifts for various combinations of the remaining sample are given in Table 5. It seems probable that the four low-velocity objects NGC 2545, UGC 4308, A0816 + 21, and NGC 2565, all of which lie close together on one side of the cluster, are members of a foreground group, the existence of which was first discussed by Tifft, Jewsbury, and Sargent (1973). In addition, NGC 2570 is a likely background object—its velocity is greater than 3 σ from the mean cluster redshift whether or not the foreground group is

[5] The brightest spiral in Virgo listed in the RC2 is NGC 4321 with $B_T = 10.10$ mag. However, both NGC 4501 ($B_T = 10.27$ mag) and NGC 4569 ($B_T = 10.23$ mag) probably become brighter than NGC 4321 after correction is made for internal absorption.

TABLE 4*a*

PEGASUS I REDSHIFTS[a]

Name: UGC	Name: Other	Type	m_{Zw} (mag)	V(opt)[b] (km s^{-1})	σ_V (km s^{-1})	Source[c]	V(H I)[b,d] (km s^{-1})	Source[c]	V_0 (km s^{-1})
---	Z406-005[e]............	S[f]	15.3	4893	100	2	---	---	5094
---	Z406-009............	E[f]	15.5	6404	100	2	---	---	6607
12407	---	S	14.2	6574	100	2	---	---	6781
12417	IC 1474.............	Sc	14.9	3371	100	2	3471	1	3665
12422	NGC 7518, Mk 527.....	Sa	14.5	3510	75	2,3,4	3531	1	3727
12423	---	Sc	14.8	4813	100	2,4	4850	1	5046
12431	NGC 7529............	S	14.6	4570	100	2	4552	1	4757
12442	NGC 7537............	Sb	13.8	2650	50	2,4,5	2679	1,11	2868
12447	NGC 7541............	Sc	12.7	2500	200	4,6	2675	1,10,11	2864
---	Z406-031............	S[f]	15.7	4648	150	12	---	---	4848
12454	---	S0	15.0	4758	100	2	---	---	4965
---	NGC 7557............	E[f]	15.0	3612	100	4	---	---	3808
12464	NGC 7562............	E	13.0	3620	150	4,6	---	---	3816
12472	---	S0	14.8	6513	100	2	---	---	6716
---	NGC 7583............	E[f]	15.2	3781	100	2	---	---	3979
12486	NGC 7591............	Sb	13.8	5002	100	2	4950	1,11	5144
---	Z406-058............	E[f]	14.9	4946	100	2	---	---	5142
12494	---	Sc	15.0	4238	100	2	4181	1	4376
12497	---	Ir	15.6	---	---	---	3759	1	3957
12498	IC 5309.............	Sb	15.0	4264	100	2	4162	1	4361
12500	NGC 7608............	S	15.2	3561	100	2	3480[g]	1	3680
12509	NGC 7611............	S0	14.0	3331	100	2,6	---	---	3530
12511	NGC 7610............	Sc dis	14.9	3506	75	7	3550	1,7	3756
12512	NGC 7612............	S0	14.3	3189	100	2	---	---	3390
---	NGC 7617............	S0:	15.1	4072	200	6	---	---	4271
12522	---	S dwf	16.5	---	---	---	2798	1	2997
12523	NGC 7619............	E	12.7	3757	200	6	---	---	3956
12526	NGC 7623............	S0	13.9	3463	200	6	---	---	3663
12531	NGC 7626............	E	12.8	3531	100	6,8	---	---	3730
---	Z406-078............	E-S0[f]	14.8	3074	100	2	---	---	3270
12539	NGC 7631............	Sb	13.8	3773	100	2	3742	1,11	3941
12542	NGC 7634............	SB0	13.7	3219	75	2,9	---	---	3420
---	Z406-086............	S	15.5	3602	100	2	3575	1	3776
12544	---	IB(s)m	15.5	---	---	---	2849	1	3051
12575	NGC 7648, Mk 531.....	S0	13.5	3700	150	2,3	---	---	3903
12602	NGC 7671............	S0	14.3	4150	75	2,4,6	---	---	4360
---	NGC 7672............	Sb	14.8	4393	200	4	---	---	4603

[a]Only galaxies in the redshift range 1000-7000 km s^{-1} (after correction for solar motion) are compiled here.

[b]Heliocentric velocities.

[c]Redshift sources are (1) Schommer, Sullivan, and Bothun (1980); (2) Chincarini and Rood (1976); (3) Kopylov *et al*. (1974); (4) Turner (1976); (5) de Vaucouleurs and de Vaucouleurs (1967); (6) Humason, Mayall, and Sandage (1956); (7) Rubin *et al*. (1976); (8) Disney and Cromwell (1971); (9) Barbon and Capaccioli (1974); (10) Shostak (1978); (11) Krumm and Salpeter (1979); (12) Kowal and Sargent (1971).

[d]Unless otherwise noted, a nominal error of ±20 km s^{-1} is adopted for V(H I).

[e]Z406-005 is within Pegasus II contour of Zwicky *et al*. (1961-1968); however, we assign its membership to the Pegasus I cluster.

[f]Types assigned by present authors.

[g]Error = ±40 km s^{-1}.

TABLE 4*b*

CANCER REDSHIFTS

UGC	Name Other	Type	m_{Zw} (mag)	V(opt)[a] (km s^{-1})	σ_V (km s^{-1})	Source[b]	V(H I)[a,c] (km s^{-1})	Source[b]	V_0 (km s^{-1})
4287	NGC 2545.............	S	13.2	3400	150	2,3	---	---	3302
4308	---	SBc	14.5	---	---	---	3631	1	3534
4312	NGC 2554.............	S0-a	13.5	4163	100	2	---	---	4074
4324	---	S	15.3	4801	100	4	---	---	4699
4329	---	Sc	15.0	---	---	---	4092	1	3992
4330	NGC 2557.............	S0	14.6	4944	100	4	---	---	4845
4331	NGC 2558.............	Sa-b	14.6	---	---	---	4979	1	4876
---	A0816.5+2110.........	S[d]	16.2[d]	3728	100	5	---	---	3627
---	Z119-053.............	S	15.5	4720	100	5	4852	1	4751
4332	---	Pec	15.5	5506	100	5	---	---	5405
4334	NGC 2565, Mk 386.....	Sb	13.8	3510	100	2,5,11	3583	1	3487
4337	NGC 2560.............	S0-a	14.9	4903	100	4	---	---	4802
---	Z119-059.............	S	15.7	4274	100	5	---	---	4173
---	Z119-061.............	S	15.5	5181	100	5	---	---	5080
4344	---	S	15.5	5008	150	11	5030	1	4928
4345	NGC 2562.............	S0-a	14.0	4963	200	6	---	---	4862
4347	NGC 2563.............	S0	13.7	4501	150	5,6	---	---	4400
---	A0817.7+2114.3.......	E[d]	16.2[d]	4674	100	5	---	---	4573
---	A0817.9+2112.8.......	E[d]	16.0[d]	4542	100	5	---	---	4441
4354	NGC 2570.............	Sa-b	15.4	---	---	---	6541	1	6439
4367	NGC 2577.............	E-S0	13.8	2123	100	4	---	---	2029
4375	---	Sc	14.6	---	---	---	4374	1	4280
4383	IC 2338+2339.........	S,S	14.7[e]	5215[f]	100	4	5348[g]	1,7	5248
4384	IC 2341..............	E-S0	14.9	4846	100	2	---	---	4746
4386	---	Sb	14.8	---	---	---	4649	1	4547
4391	NGC 2582.............	Sb	14.3	4455	75	2,8	---	---	4350
4399	---	S-Ir	15.5	4349	?	11	5344	12	5244
4409	IC 2373..............	Sc?	15.5	---	---	---	7507	1	7402
4422	NGC 2595.............	SBb/Sc	13.9	4355	100	2,9,10	4332	1	4232
4458	NGC 2599, Mk 389.....	Sa	13.4	4690	100	2	4732	1	4637

[a]Heliocentric velocities.

[b]Redshift sources are (1) Schommer, Sullivan, and Bothun (1980); (2) Chincarini and Rood (1972); (3) Sandage (1978); (4) Kintner (1971); (5) Tifft, Jewsbury, and Sargent (1973); (6) Humason, Mayall, and Sandage (1956); (7) Peterson and Shostak (1974); (8) Rubin *et al*. (1976); (9) Sargent (1970); (10) Barbon (1969); (11) Kowal and Sargent (1971); (12) this paper.

[c]Unless otherwise noted, a nominal error of ±20 km s^{-1} is adopted for V(H I).

[d]Magnitude and type adopted from Tifft, Jewsbury, and Sargent (1973).

[e]Combined magnitude.

[f]Mean of V = 5230 km s^{-1} (IC 2338) and V = 5194 km s^{-1} (IC 2339).

[g]Error = ±30 km s^{-1}.

1980ApJ...239...12A

TABLE 4c

ZWICKY 74-23 REDSHIFTS

Name			m_{Zw}	V(opt)[a]	σ_V		V(H I)[a,c]		V_0
UGC (1)	Other (2)	Type (3)	(mag) (4)	(km s^{-1}) (5)	(km s^{-1}) (6)	Source[b] (7)	(km s^{-1}) (8)	Source[b] (9)	(km s^{-1}) (10)
8878[d]	---	SBb	14.5	---	---	---	6833	2	6809
8918	---	S	14.8	---	---	---	4101	1,2	4075
---	Z74-035......	Sc	15.6	---	---	---	4609[e]	1,2	4582
---	Z74-039......	Sc[f]	15.3	---	---	---	6844	1	6824
8938	NGC 5409.....	Sb/SBb	14.4	---	---	---	6258	1,2	6236
---	Z74-45.......	Sb	14.7	6276	100	3	6068	1,2	6043
8940	NGC 5411.....	E-S0	14.6	5850	100	3	---	---	5826
8942	NGC 5414.....	Pec	14.2[g]	4224	100	3	4279	2	4259
8944	NGC 5416.....	Sc	13.6	6183	50	3,4	6235	1,2	6213
8948	---	SBb	15.0	---	---	---	6005	1,2	5982
8950	---	Sc	15.7	---	---	---	5859	1,2	5836
8951	---	Sc	15.6	---	---	---	5865	1,2	5841
8952	NGC 5423.....	E-S0	13.9	5785	50	3,4	---	---	5763
8956	NGC 5424.....	S0	14.3	5900	150	3,4	---	---	5878
---	NGC 5431.....	Sd[f]	14.8	5745	200	3	---	---	5723
8965	NGC 5434.....	Sc	14.3	---	---	---	4634	1,2	4613
8967	---	Sb-c	14.7	5550	100	3	5637	1,2	5616
8971	NGC 5436.....	S0/a	14.9	6614	200	3	---	---	6593
---	NGC 5438.....	E[f]	14.7	7066	100	3	---	---	7046
9007	---	Sdm	15.6	---	---	---	4600	2	4580
---	Z74-096......	Ir	15.3	---	---	---	7044	2	7022
9015	---	S	15.2	---	---	---	7001	2	6980
9023	---	Sc	15.4	---	---	---	7208	2	7189

[a] Heliocentric velocities.

[b] Redshift sources are (1) Sullivan *et al.* (1980); (2) Chincarini, Giovanelli, and Haynes (1980); (3) Thompson, Welker, and Gregory (1978); (4) Davis *et al.* (1979).

[c] Unless otherwise noted, a nominal error of ±20 km s^{-1} is adopted for V(H I).

[d] Galaxy is just outside the contour of Zwicky *et al.* (1961-1968) but within cluster bounds following Thompson, Welker, and Gregory (1978).

[e] The small redshift (4363 km s^{-1}) and large velocity width (620 km s^{-1}) quoted by Chincarini, Giovanelli, and Haynes (1980) appear to be due to a spurious noise feature. If the feature is ignored, the redshift and velocity width then agree well with that given in Sullivan *et al.* (1980).

[f] Type from Thompson, Welker, and Gregory (1978).

[g] Magnitude following Chincarini, Giovanelli, and Haynes (1980).

TABLE 5

MEAN CLUSTER REDSHIFTS

Sample	N	Equal Weights $\langle V_0 \rangle$ (km s^{-1})	Equal Weights σ (km s^{-1})	Equal Weights σ_μ (km s^{-1})	Luminosity Weighted $\langle V_0 \rangle$ (km s^{-1})	Luminosity Weighted σ (km s^{-1})	Luminosity Weighted σ_μ (km s^{-1})
Pegasus I							
Total	34	3992	665	114	3816	620	106
NGC 7537, 7541 excluded	32	4062	619	109	3983	509	90
E-S0	15	3947	543	140	3841	371	96
Spirals (NGC 7537, 7541 excluded)	17	4163	679	165	4303	634	154
All spirals	19	4027	760	174	3781	871	200
Cancer							
Total	28	4556	657	124	4326	645	122
NGC 2570 excluded	27	4486	554	107	4293	591	114
NGC 2570 and possible foreground group excluded	23	4660	384	80	4559	362	76
Possible foreground group	4	3488	137	68	3404	125	62
E-S0	5	4601	192	86	4566	483	97
Spirals (NGC 2570 and foreground group excluded)	18	4677	425	100	4561	391	92
All spirals	23	4546	723	151	4289	687	143
Zwicky 74-23							
Total	23	5893	932	194	5844	879	183
Possible foreground group excluded	18	6301	545	128	6222	491	116
Possible foreground group and background groups excluded	12	5963	272	79	5985	265	76
Possible foreground group	5	4422	242	108	4389	240	107
Possible background group	6	6978	144	59	6959	142	58
Perseus Supercluster							
Galaxies, this paper	13	5557	756	210	5508[a]	697	193
Mean chain redshift	116	5164	706	69	---	---	---

[a] Weighted by $H_{-0.5}$

included. The mean difference $\langle V_{\rm optical} - V_{\rm H\,I} \rangle = -63 \pm 25$ km s^{-1} for six galaxies (excluding the anomalous case of UGC 4399).

Z74-23.—Redshifts for a total of 23 galaxies are given in Table 4*c*, and the velocity distribution is shown in Figure 2*c*. Once again the cluster membership is somewhat ambiguous. Figure 2*c* suggests that the cluster may actually break up into three groups. However, except for the fact that three of the five high-velocity galaxies (Z74-096, UGC 9015, and UGC 9073) lie close together, there is no pronounced spatial segregation of objects. Examination of Zwicky field 74 reveals a large number of galaxies spread uniformly about, but with a clear concentration around NGC 5416. It seems that additional redshifts will be needed to clarify the situation.

The mean redshifts for various combinations of the data are given in Table 4. Note the rather large velocity dispersion ($\sigma = 881$ km s^{-1}) that results if the sample is considered in its entirety. The mean difference $\langle V_{\rm optical} - V_{\rm radio} \rangle = 4 \pm 69$ km s^{-1} for four galaxies.

Perseus supercluster.—H I velocities from Bania, Thompson, and Thuan (1980) for our full sample are given in Table 2. The mean redshift of $\langle V_0 \rangle = 5508 \pm 197$ km s^{-1} (Table 4) agrees well with the mean redshift of the Perseus cluster itself, $\langle V_0 \rangle = 5460 \pm 200$ km s^{-1} (Chincarini and Rood 1971), although it is somewhat larger than that for the chain as a whole for which $\langle V_0 \rangle = 5164 \pm 69$ km s^{-1} (Gregory, Thompson, and Tifft 1980).

VI. DISTANCE SCALE BEYOND THE LOCAL SUPERCLUSTER

a) *Cluster Loci and Hubble Ratios*

Infrared Tully-Fisher diagrams for the four samples considered here are shown in Figure 3. The fitted lines in the figure have a slope equal to 10, close to the mean slope for the whole sample (Paper I). It is clear that each cluster populates a well-defined locus in the Tully-Fisher diagram over a range of $\sim$2–5 mag. The dispersion about the mean relations is somewhat larger than that seen in the nearby samples (Papers I and II), but this is not surprising given the lower S/N of the present limiting data.

A distance modulus for each galaxy is given in Table 6 and was calculated by first deriving the absolute $H_{-0.5}$ magnitude from the relation

$$H_{-0.5}{}^{\rm abs} = -21.23 - 10[\log \Delta V_{20}{}^c(0) - 2.5]\,. \quad (8)$$

The zero point of this equation is based solely on

TABLE 6

DISTANCE MODULI OF GALAXIES

Name	$H_{-0.5}$ (mag)	$H^c_{-0.5}$ (mag)	$\Delta V^c_{20}(0)$ (km s^{-1})	$H^{abs}_{-0.5}$ (mag)	$m-M$ (mag)	r (Mpc)	V_0/r (km s^{-1} Mpc^{-1})
			Pegasus I				
UGC 12417......	11.90	11.87	308	-21.12	32.99	39.6	92.6
UGC 12423......	10.88	10.84	526	-23.44	34.28	71.8	70.3
UGC 12442......	10.78	10.76	354	-21.72	32.48	31.3	91.6
UGC 12447......	9.10	9.08	488	-23.11	32.19	27.4	105
UGC 12486......	10.40	10.36	463	-22.89	33.25	44.7	115
UGC 12494......	13.45	13.42	260	-20.38	33.80	57.5	76.1
UGC 12497......	13.83[a]	13.80	208	-19.41	33.21	43.9	90.1
UGC 12498......	11.65	11.62	310	-21.14	32.76	35.6	123
UGC 12539......	10.74	10.71	412	-22.38	33.09	41.5	95.0
Z406-086.......	13.44[b]	13.41	220	-19.65	33.06	40.9	92.3
			Cancer				
UGC 4329.......	11.53	11.49	299	-20.99	32.48	31.3	128
Z119-053.......	12.98	12.93	290	-20.85	33.78	57.0	83.4
UGC 4334.......	9.89	9.85	462	-22.88	32.73	35.2	99.1
UGC 4354.......	12.29	12.23	355	-21.73	33.96	61.9	104
UGC 4386.......	10.67	10.62	516	-23.36	33.98	62.5	72.8
UGC 4399.......	13.03	12.98	280	-20.70	33.68	54.5	96.2
			Zwicky 74-23				
UGC 8918.......	11.79	11.76	334	-21.47	33.23	44.3	92.0
UGC 8938.......	11.29	11.25	450	-22.76	34.01	63.4	98.4
UGC 8942.......	11.71	11.68	427	-22.53	34.21	69.5	61.3
UGC 8944.......	11.21	11.17	400	-22.25	33.42	48.3	129
UGC 8948.......	11.95	11.91	404	-22.29	34.20	69.2	86.4
UGC 8950.......	14.48[c]	14.44	202	-19.28	33.72	55.5	105
UGC 8951.......	13.92	13.88	261	-20.40	34.28	71.8	81.4
UGC 8967.......	11.72	11.68	380	-22.04	33.72	55.5	101
UGC 9023.......	13.86	13.81	282	-20.73	34.54	80.9	88.9
			Perseus Supercluster				
UGC 94.........	10.99	10.95	439	-22.65	33.60	52.5	91.9
UGC 98.........	11.35	11.30	371	-21.92	33.22	44.1	114
UGC 100........	11.07	11.02	438	-22.64	33.66	54.0	93.3
UGC 238........	11.28	11.22	431	-22.57	33.79	57.3	122
UGC 255........	11.42	11.37	429	-22.55	33.92	60.8	107
UGC 279........	11.32	11.27	460	-22.86	34.13	67.0	97.1
UGC 433........	11.32	11.28	435	-22.61	33.89	60.0	81.3
UGC 562........	10.10	10.05	503	-23.25	33.30	45.7	124
UGC 927........	11.79	11.74	365	-21.85	33.59	52.2	119
UGC 979[d].......	(10.32)	(10.27)	526:	-23.44:	(33.71)	(55.2)	(90.5)
UGC 1577[e]......	10.72	10.67	(414)	(-22.40)	(33.07)	(41.1)	(132)
UGC 1835.......	10.81	10.76	436	-22.62	33.38	47.4	110
UGC 2134.......	10.96	10.92	387	-22.11	33.03	40.4	116
UGC 2274.......	10.82	10.76	475	-23.00	33.76	56.5	95.6
UGC 12666......	12.38	12.33	347	-21.63	33.96	61.9	84.7

[a] Extrapolation of galaxy growth curve and mean Sc curve both give 13.83.

[b] Magnitude extrapolated using mean Sc growth curve.

[c] Value is mean of H = 14.45 mag (from extrapolation of two largest aperture measurements) and H = 14.50 (obtained from smallest aperture measurement).

[d] Morphologically peculiar; weight = 0 assigned.

[e] Very uncertain inclination; weight = 0 assigned.

Sandage-Tammann distances to M31 and M33, adopting a Hyades modulus of 3.29 mag (see Paper I). In Table 6 the distance modulus (col. [6]) is simply the difference between columns (3) and (5). The final two columns in Table 6 give the distance and resulting values of the Hubble ratio, using the individual galaxy redshifts from Table 4.

In Table 7 we present mean distance moduli and Hubble ratios. Various combinations are considered in view of the cluster membership ambiguities discussed

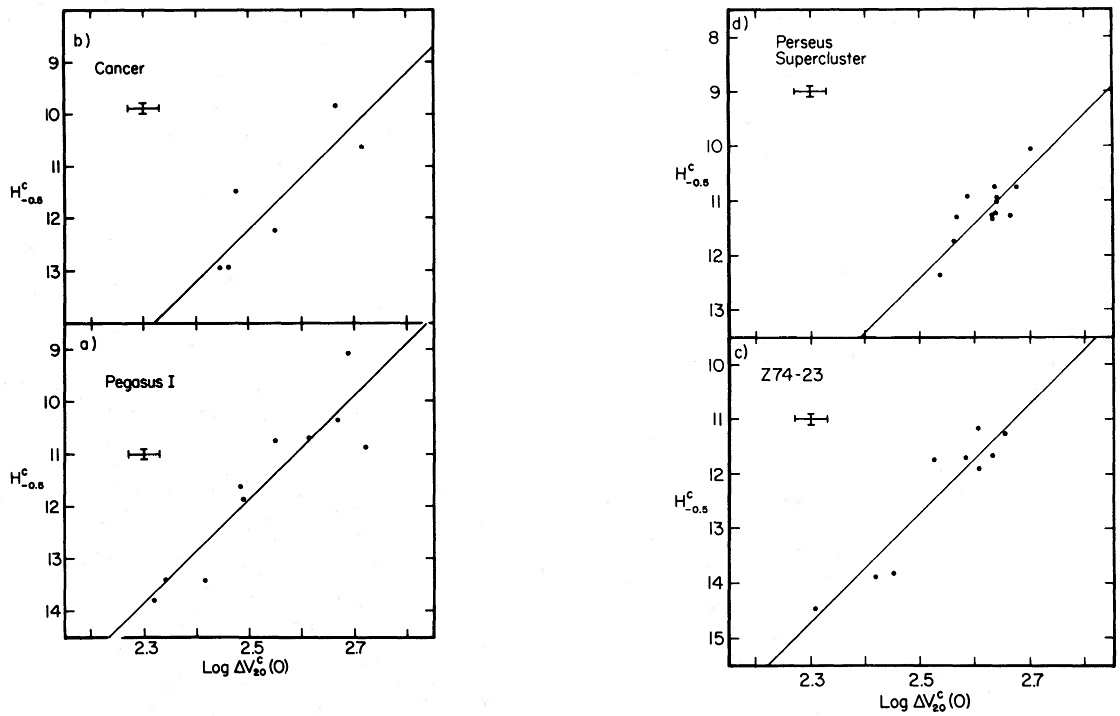

FIG. 3.—IR Tully-Fisher diagrams from the fully corrected data in Table 6. The equation of the fitted line is given by $H_{-0.5}{}^{c-} = a + 10[\log \Delta V_{20}{}^{c}(0) - 2.5]$, where a = 11.88 mag for Pegasus I, 12.21 mag for Cancer, 12.70 mag for Z74-23, and 12.40 mag for the Perseus supercluster. These fits are determined from the "total" samples (see text). Nominal errors of 0.1 mag and 0.03 dex are also shown.

TABLE 7
HUBBLE RATIOS BEYOND THE LOCAL SUPERCLUSTER

Sample	N	⟨m−M⟩ (mag)	⟨r⟩ (Mpc)	⟨V_0⟩/⟨r⟩ (km s^{-1} Mpc^{-1})	⟨V_0/r⟩ (km s^{-1} Mpc^{-1})
Pegasus I					
Total	10	33.11±0.19	41.9± 3.7	91.1± 8.4	95.1± 5.1
Restricted (NGC 7537, 7541 excluded)	8	33.31±0.18	45.9± 3.8	86.8± 7.4	94.3± 6.3
NGC 7537, 7541	2	32.34±0.15	29.4± 2.0	97.4± 6.6	98.3± 6.7
Cancer					
Total	6	33.44±0.27	48.8± 6.1	88.6±11.4	97.3± 7.7
UGC 4354 (possible background) excluded	5	33.33±0.30	46.3± 6.4	92.7±13.0	95.9± 9.3
Restricted (UGC 4354 and 4334 [possible foreground] excluded)	4	33.48±0.34	49.7± 7.8	91.7±14.5	95.1±12.0
UGC 4334	1	32.73±0.4	35.2± 6.5	96.7±17.9	99.1
UGC 4354	1	33.96±0.4	61.9±11.4	---	104
Zwicky 74-23					
Total	9	33.93±0.14	61.1± 3.9	95.6± 6.8	93.7± 6.2
UGC 8918 and 8942 (possible foreground) excluded	7	33.98±0.15	62.5± 4.3	100 ± 7.1	98.6± 6.0
Restricted (UGC 8918, 8942, and 9023 [possible background] excluded)	6	33.89±0.13	60.0± 3.6	99.7± 6.1	100 ± 6.8
UGC 8918, 8942	2	33.72±0.49	55.5±12.6	79.1±17.9	76.7±15.2
UGC 9023	1	34.54±0.04	80.9±14.9	86.0±15.9	88.9
Perseus Supercluster					
Redshifts, this paper	13	33.63±0.09	53.2± 2.2	104 ± 5.6	104 ± 4.0
Mean supercluster redshift				97.1± 4.1	

in § V. Note that the quantity $\langle V_0\rangle/\langle r\rangle$ is obtained from column (4) of Table 7 and the mean cluster redshifts given in Table 5, while $\langle V/r\rangle$ is calculated from the individual galaxies (last col. in Table 6). Presumably, $\langle V_0\rangle/\langle r\rangle$ is the best Hubble ratio to use for a bound cluster; on the other hand, $\langle V_0/r\rangle$ is perhaps more appropriate for the Perseus supercluster. The quoted errors in Table 7 represent only the internal dispersion about these means. The results for the individual clusters are briefly discussed below.

Pegasus I.—A Hubble ratio of 91 ± 8 km s^{-1} Mpc^{-1} is obtained from the total sample, and one of 87 ± 7 km s^{-1} Mpc^{-1} is found if NGC 7537 and 7541 are excluded. Our distances to NGC 7537 and 7541 support the view that the pair is foreground to the cluster. One additional object is worth special mention, UGC 12423, the largest diameter spiral in the cluster.[6] The object has a high axial ratio $a/b \approx 9$. The hydrogen-mass–to–blue-luminosity ratio M_H/L_B is also large (Schommer, Sullivan, and Bothun 1980). A recent KPNO 4 m plate taken by Bruce Carney (1979) reveals the presence of substantial warping in the outer disk. These facts may be relevant to the discrepant location of this galaxy in the Tully-Fisher diagram (Table 6 and Fig. 3).

Cancer.—The full sample leads to a Hubble ratio of 89 ± 11 km s^{-1} Mpc^{-1}. Restricting the sample to certain cluster members gives 92 ± 14 km s^{-1} Mpc^{-1}. Our distance to UGC 4354 is consistent with its being a background member (§ V). Similarly, our distance to UGC 4334, a member of the possible foreground group discussed in § V, is consistent with the existence of such a group.

Z74-23.—The full sample yields 96 ± 7 km s^{-1} Mpc^{-1}, and a sample restricted to the 6000 km s^{-1} clump (Fig. 2) gives 100 ± 7 km s^{-1} Mpc^{-1}. Two of the galaxies (UGC 8918 and 8942) are in the possible foreground group, and one (UGC 9023) is in the possible background group. Our distances to the suspected nonmembers are again consistent with the existence of these groups.

Perseus supercluster.—The Hubble ratios obtained are in the range 97–104 km s^{-1} Mpc^{-1}. Three of the galaxies in Table 6 belong to the Pisces cluster proper (UGC 562, 927, and 979), while the remaining objects are drawn from the intercluster region, as discussed in § II. Because of the morphological peculiarity of UGC 979 (see Table 3) and the very uncertain inclination of UGC 1577, these galaxies have not been included in the final distance determination.

If the supercluster galaxies partake in the Hubble flow, a correlation would be expected between distance and velocity. Such a correlation is, in fact, visible in Figure 4, where distance moduli from Table 6 are plotted against log V_0 from Table 2. The correlation coefficient for Figure 4 is 0.54, increasing to 0.63 if the

[6] After correction for inclination effect, log d for NGC 7541 is slightly larger than for UGC 12423 (Table 3), but, as discussed, NGC 7541 is a probable foreground galaxy.

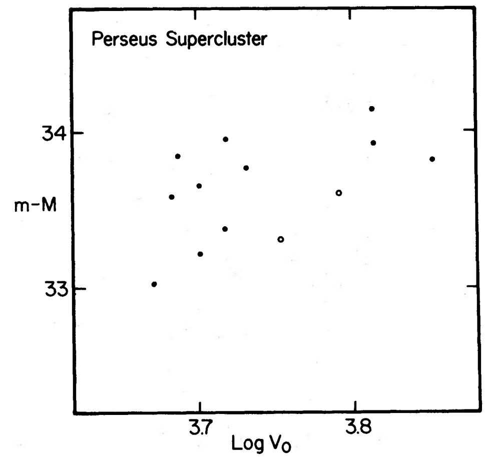

FIG. 4.—Distance moduli from Table 6 vs. corrected velocities from Table 2 for galaxies in the Perseus supercluster. Two members of the Pisces cluster proper are denoted by open circles.

two Pisces galaxies UGC 562 and 927 and eliminated. Figure 4 suggests that the depth of the supercluster chain is less than ~ 0.8 mag, corresponding to a depth of $\lesssim 20$ Mpc at our distance of 53 Mpc. We deduce that the length-to-depth ratio of the chain is greater than 3, similar to the length-to-width ratio. Our results thus support the filamentary picture of the chain discussed by Gregory, Thompson, and Tifft (1980). The implications with regard to formation of large-scale structure in the universe deserve further study (e.g., Zel'dovich 1978).

b) Velocity Perturbation and Global Value of H_0

An unweighted mean of the Hubble ratios $\langle V_0\rangle/\langle r\rangle$ for the four "total" samples gives 95 ± 3 km s^{-1} Mpc^{-1}; considering only the restricted samples which exclude all possible foreground and background groups, the result is 96 ± 4 km s^{-1} Mpc^{-1}. Finally, the mean unweighted $\langle V_0/r\rangle$ value for the four samples is 98 ± 3 km s^{-1} Mpc^{-1}. Recall that in Paper II a Hubble ratio of 65 ± 4 km s^{-1} Mpc^{-1} was obtained for the Virgo cluster. The difference of $\sim 30 \pm 6$ km s^{-1} Mpc^{-1} between this value and that obtained from the distant clusters is, therefore, significant at a level of $\sim 5\,\sigma$, irrespective of any ambiguities in cluster membership or difficulties in calibrating the *absolute* distance scale.

The simplest way to account for this discrepancy is to postulate a component of Local Group motion in the direction of Virgo itself. With this assumption and a uniform Hubble flow outside the Local Supercluster, the velocity perturbation ΔV in the direction of Virgo is given by

$$\Delta V = \Delta H\left(\frac{1}{r_{\rm Virgo}} - \frac{\cos\theta}{r}\right)^{-1} . \quad (9)$$

In this equation ΔH is the difference in Hubble ratio between Virgo and a more distant cluster, $r_{\rm Virgo}$ and r

TABLE 8

ESTIMATES OF ANISOTROPIC MOTION AND THE GLOBAL VALUE OF H_0[a]

Cluster	N	Hubble Ratio (km s^{-1} Mpc^{-1})	ΔH (km s^{-1} Mpc^{-1})	cos θ	ΔV (km s^{-1})	H_0[b] (km s^{-1} Mpc^{-1})	V_c (km s^{-1} Mpc^{-1})	H_0[c] (km s^{-1} Mpc^{-1})
			Total Sample					
Virgo............	19	65.3[g]	---	---	---	---	1461	93.7
Pegasus I.........	10	91.1	25.8	-0.896	302	84.7	3421	81.6
Cancer...........	6	88.6	23.3	0.513	435	93.2	4553	93.3
Zwicky 74-23......	9	95.6	30.3	0.916	617	105	6248	102
Perseus Supercluster[d]...	13	97.1	31.8	-0.671	415	91.9	4867	91.5
Mean.............					442±65	93.7±4.2		92.4±3.2
			Restricted Sample					
Virgo............	19	65.3[g]	---	---	---	---	1508	96.7
Pegasus I.........	8	86.8	21.5	-0.896	257	81.8	3548	77.3
Cancer...........	4	91.7	26.4	0.513	491	96.8	4810	96.8
Zwicky 74-23......	6	99.7	34.4	0.916	704	110	6433	107
Perseus Supercluster[d]...	13	104	38.7	-0.671	504	97.6	5180	97.7
Mean.............					489±91	96.6±5.8		95.1±4.9
			⟨V/r⟩ Sample					
Virgo............	19	65.3[g]	---	---	---	97.8[e]		
Pegasus I.........	10	95.1	29.8	-0.896	349[f]	87.7		
Cancer...........	6	97.3	32.0	0.513	597[f]	104		
Zwicky 74-23......	9	93.7	28.4	0.916	578[f]	102		
Perseus Supercluster[d]...	13	104	38.7	-0.671	504[f]	97.6		
Mean.............					507±56	97.8±2.8		

[a] Distance and redshift of 15.6 Mpc and 1019 km s^{-1} adopted for Virgo; other distances and redshifts adopted from Tables 6 and 7. See text for further details.

[b] Global value obtained from individual cluster.

[c] Global value obtained assuming ΔV = 442 km s^{-1} (for Total Sample), and ΔV = 489 km s^{-1} (for Restricted Sample).

[d] Position of UGC 927 ($01^h20^m.4$, +33°17') in Pisces cluster is adopted for these calculations.

[e] ΔV = 507 km s^{-1} adopted for Virgo.

[f] Mean distance of total sample assumed.

[g] From Paper II

are the distance to Virgo and the more distant cluster, respectively, and θ is the great circle angle between Virgo and the more distant cluster. Various estimates of ΔV are given in Table 8, where we have considered separately the total and restricted samples and $\langle V/r \rangle$ calculation for each individual cluster. For these calculations, we have used a Virgo modulus and distance[7] of 30.96 mag and 15.6 Mpc. From the mean of the results in Table 8, we obtain a value of

$$\Delta V = 480 \pm 75 \text{ km s}^{-1} \quad (10)$$

for the Local Group motion toward Virgo.

The values of ΔV and H_0 given in columns (6) and (7) of Table 8 are the velocity perturbation and expansion rate implied by the difference between the Hubble ratio for Virgo and each cluster individually (eq. [9]). A further iteration was then made by first correcting the recessional velocity of each cluster for Local Group motion (using the *mean* ΔV) to obtain V_c in column (8) and then recalculating H using the corrected cluster redshifts (col. [9]). We conclude that our best estimate for the value of the Hubble constant is

$$H_0 = 95 \pm 4 \text{ km s}^{-1} \text{ Mpc}^{-1} . \quad (11)$$

This result should be considered preliminary in the sense that we are presently obtaining distances to many more galaxies in the present cluster sample and in additional distant clusters. The formal error in equation (11) does not include the uncertainty arising from Local Group distance moduli which we estimate to be 0.2 mag (see Paper I), or 10% in H_0. If a zero point based on de Vaucouleurs's (1978) distances to M31 and M33 is adopted instead, all moduli here *decrease* by 0.41 mag, or 18% in distance, and the expansion rate increases by a similar amount (see Paper I).

[7] The value of 30.98 mag from Paper II has been adjusted downward by 0.02 mag in view of equations (1) and (7) of this paper.

However, the value we obtain for the velocity perturbation ΔV is irrespective of adopted zero point.

VII. POSSIBLE SYSTEMATIC ERRORS

In this section we examine evidence for systematic errors which might lead to the difference in Hubble ratio between Virgo and the more distant clusters.

a) Measurement Errors

i) *Infrared Magnitudes*

To account for a difference of $\Delta H = 30$ km s^{-1} Mpc^{-1}, a systematic error of 0.8 mag must be present. There is simply no evidence for any such effect in the magnitudes. In particular, the photometry in this paper was taken with various combinations of detectors, filters, photometers, and telescopes. The agreement between observations made with different systems is generally well within the statistical errors.

ii) *Velocity Widths*

Alternatively, an error of $0.8/10 = 0.08$ in log ΔV is needed to produce our value of ΔH, which corresponds to an error of ~ 60 km s^{-1} at $\Delta V = 300$ km s^{-1}. Might a systematic error be present because most of the data in this paper were obtained at Arecibo, while most of the Virgo velocity widths in Paper II were obtained with smaller radio telescopes? There is unfortunately little in the way of direct comparison for data in the present series. We do note that Shostak's (1978) profile width for NGC 7541, obtained with the National Radio Astronomy Observatory 300 foot (90 m) telescope, is in good agreement with the Arecibo profile widths of Schommer, Sullivan, and Bothun (1980) and of Krumm and Salpeter (1979). Also, the mean difference between the Krumm and Salpeter (1979) and Helou, Salpeter, and Krumm (1979) Arecibo profile widths and those obtained with smaller telescopes for three Virgo galaxies is 3 ± 9 km s^{-1} (see Paper II).[8]

A small systematic effect presently uncorrected in the current data is due to smoothing of the original profile resolution (8 km s^{-1}) to some larger value. This means that our reported widths are slightly too large. Preliminary results indicate that for a typical profile the overestimate in ΔV_{20} is ~ 2 km s^{-1} sin i for resolution $\Delta V_s = 26$ km s^{-1} and ~ 10 km s^{-1} sin i for $\Delta V_s = 43$ km s^{-1}. The inclination of the galaxy enters, since it influences the steepness of the profile edges. In the present sample the Perseus supercluster profiles have $\Delta V_s = 16$ km s^{-1}, and most other profiles have $\Delta V_s = 43$ km s^{-1}, except for four cases where $\Delta V_s = 26$ km s^{-1}. We calculate that this bias may lead to an *underestimate* of H_0 in our distant sample of $\sim 6\%$ for $\Delta V_s = 43$ km s^{-1} and of $\sim 1.5\%$ for $\Delta V_s = 26$ km s^{-1}. (No such correction was required or applied to the calibrating or Virgo galaxies in Papers I and II.) Detailed modeling of H I profiles, now in progress, is needed before this bias can be more accurately estimated.

Finally, as the telescope-beam–to–galaxy-size ratio in Paper II and this paper are comparable in the mean, we do not expect errors due to simple variation of this ratio to be significant. Of course, as long as the beam includes V_{max}, the situation we believe to be true for virtually all the data here, this ratio is irrelevant. Furthermore, in Krumm and Salpeter's (1979) survey of galaxies closer than Virgo, only rarely are larger velocities found in off-nucleus profiles when compared with nuclear ones. We conclude that there is no evidence for significant relative velocity-width errors between Virgo and the more distant clusters.

iii) *Diameters*

A more serious possibility concerns the adopted isophotal diameters, which are heavily weighted by the eye estimates of Nilson (1973) in the UGC. Two questions are relevant. First, how linear are these estimates with changing galaxy size? For instance, a systematic overestimate by Nilson of the diameters for smaller (e.g., higher redshift) galaxies would be interpreted by us as a larger value of the Hubble constant outside the Local Supercluster. The second question is, How well do the UGC (and RC2) diameters actually correspond to isophotal diameters? For example, variations in background fog on POSS plates could lead to systematic isophotal errors.

To answer the first question, we have performed the following test. Twenty-two galaxies from Zwicky *et al.* (1961–1968) field 158 were traced with the KPNO PDS microphotometer, using a square aperture of 40 μm (2″.684). This field was chosen because it contains members of both the foreground Coma I cluster and the background Coma supercluster and thus displays galaxies with a large range in size. By using the KPNO Interactive Picture Processing System (IPPS) surface-brightness density profiles were determined along the major axis for the entire sample. Then the density above sky corresponding to the UGC diameters for the eight largest galaxies was found. The mean of these eight densities was 0.043 dex ($\sim 10\%$) above sky, as would be expected from the discussion in the RC2. Finally, "instrumental" galaxy diameters at this density were determined for the entire plate sample; we refer to these as D(PDS). In Table 9 we have listed log D(UGC) and log D(PDS) and have plotted the two quantities against each other in Figure 5. Also shown in Figure 5 are two dashed lines which illustrate the degree of systematic diameter error that would be required to produce $\Delta H = 30$ km s^{-1} Mpc^{-1}. It seems clear from Figure 5 that, first, Nilson's eye measurements are remarkably uniform, and second, the possibility of significant error owing to nonlinear UGC diameters can be excluded.

[8] The agreement in velocity widths among the various independent Arecibo observers is excellent. For instance, the mean difference in widths for five galaxies in cluster Z74-23 in common between Chincarini, Giovanelli, and Haynes (1980) and Sullivan *et al.* (1980) is 2 ± 9 km s^{-1} (Table 3), well within our nominal velocity-width error of ~ 25 km s^{-1}.

TABLE 9

COMPARISON OF UGC AND INSTRUMENTAL DIAMETERS[a] IN ZWICKY FIELD 158

Name	log D (UGC)	log D (PDS)	Δ
NGC 4274........	1.86	1.85	0.01
NGC 4062........	1.68	1.66	0.02
NGC 4414........	1.68	1.69	-0.01
NGC 4314........	1.66	1.65	0.01
NGC 4448........	1.60	1.63	-0.03
NGC 4251........	1.56	1.58	-0.02
NGC 4359........	1.56	1.57	-0.01
NGC 4245........	1.54	1.56	-0.02
UGC 7012........	1.32	1.27	0.05
UGC 7017........	1.28	1.29	-0.01
UGC 7384........	1.28	1.28	0.00
UGC 7578........	1.26	1.24	0.02
UGC 7221........	1.18	1.15	0.03
UGC 7286........	1.18	1.16	0.02
UGC 7041........	1.15	1.18	-0.03
UGC 7496........	1.15	1.14	0.01
UGC 7363........	1.11	1.14	-0.03
UGC 7471........	1.08	1.02	0.06
UGC 7437........	1.04	1.02	0.02
UGC 7615........	1.04	1.03	0.01
UGC 7064........	0.90	0.98	-0.08
UGC 7395........	0.70	0.89	-0.19
Mean, n = 22....	---	---	-0.01 ±0.05

[a]All diameters are in units of 0:1.

To test how well both RC2 and UGC diameters actually correspond to isophotal diameters, we have compared them to diameters for Virgo and Hercules galaxies determined from the plate material used by and fully described in Peterson, Strom, and Strom (1979). According to Schweizer (1976), the B_3 system in Peterson, Strom, and Strom (1979) is related to B magnitudes via $B_3 = B - 0.30(B - V)$, but we have ignored this small difference for the present purpose. Two types of isophotal diameters are available from the Peterson, Strom, and Strom (1979) material. First, there are some obtainable from a single scan made along the major axis. Second, there are "halo"-type diameters from profiles averaged along ellipticity contours of equal intensity. While these have better S/N, they are not as directly comparable with the UGC and RC2 diameters as are the single-scan profiles. In Table 10 we have listed diameters at 25th mag arcsec^2 ($B_3{}^{25}$) for Virgo and Hercules galaxies. Individual Virgo sizes are listed for only those objects with single-scan profiles. While many more Hercules galaxies are analyzed by Peterson, Strom, and Strom (1979), unfortunately only four are in either the UGC or the RC2.

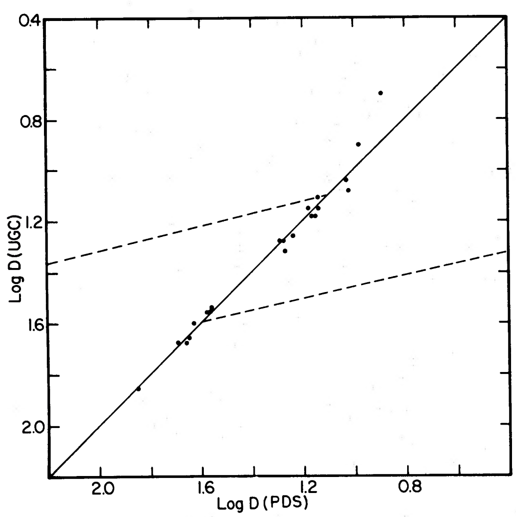

FIG. 5.—Galaxy diameters from the UGC vs. instrumental POSS diameters determined with a PDS microdensitometer (units of 0:1). The solid line has a slope of unity. The lower dashed line shows the amount by which the UGC diameters of small (e.g., more distant) galaxies would have to be overestimated in order to account for the 30 km s^{-1} Mpc^{-1} change in Hubble ratio discussed in this paper. Similarly, the upper dashed line shows the amount by which nearby galaxy diameters would have to be underestimated in order to account for the change.

Also listed in Table 10 are $B_3{}^{25}$ diameters for four Cancer cluster galaxies determined from a plate kindly loaned by Steve and Karen Strom. A section of this plate was traced with the KPNO PDS microphotometer with a 50 μm (0".928) square aperture, and the digitized picture was converted to relative intensity by using a calibration wedge of 16 steps. Absolute calibration was based on multiaperture photometry of NGC 2562 and 2563 taken from Sandage (1973). This permitted the photometric zero point to be defined with an rms error of 0.04 mag.

In Figure 6 we have plotted log $B_3{}^{25}$ against both log D_{RC2} and log D_{UGC}; the latter are also listed in Table 10. Note that the values of D_{UGC} have now been

TABLE 10

COMPARISON OF ISOPHOTAL DIAMETERS[a]

Name	Log B_3^{25}	Log D_{UGC}	Log D_{RC2}	ΔB_3^{25}-UGC	ΔB_3^{25}-RC2
Cancer Cluster					
NGC 2560............	1.24	1.19	1.24	0.05	0.00
UGC 4332............	1.22	1.16	1.22	0.06	0.00
NGC 2562............	1.11	1.13	1.14	-0.02	-0.03
NGC 2570............	1.08	1.13	---	-0.05	---
Mean................	---	---	---	0.01±0.05	-0.01±0.02
Hercules Cluster					
UGC 10195...........	1.23	1.24	---	-0.01	---
NGC 6045............	1.12	1.07	1.12	0.05	0.00
IC 1173.............	1.03[b]	1.07	1.10	-0.04	-0.07
IC 1189.............	0.89[b]	---	0.79		0.10
Mean................	---	---	---	0.00±0.05	0.01±0.09
Virgo Cluster					
NGC 4388............	1.78	1.76	1.71	0.02	0.07
NGC 4330............	1.64	1.63	---	0.01	---
NGC 4402............	1.63	1.56	1.61	0.07	0.02
NGC 4313............	1.58	1.53	1.59	0.05	-0.01
NGC 4425............	1.42	1.46	1.53	-0.04	-0.11
IC 3311.............	1.29	1.33	---	-0.04	---
IC 3099.............	1.28	1.33	---	-0.05	---
IC 3371.............	1.24	1.29	---	-0.05	---
IC 3453.............	1.20	1.13	1.09	0.07	0.11
IC 3105.............	1.19	1.26	---	-0.07	---
Mean................				0.00±0.05	0.02±0.08
Mean, "halo"-type... diameters.........				-0.03±0.04 (n = 19)	-0.01±0.04 (n = 18)

[a]All diameters in units of 0ʹ.1.

[b]"Halo"-type diameter (see text).

transformed to the RC2 system according to the prescription in that reference. Also shown in Figure 6 are dashed lines which again indicate the type of systematic error required to account for our measured value of ΔH. We conclude that both UGC and RC2 diameters accurately reflect true isophotal measurements for galaxies in Paper II and this paper.

We cannot completely dismiss the possibility of diameter errors in the very large nearby galaxies of Paper I. However, such errors would affect only the absolute scale and not the velocity perturbation measured here. We do note that the good agreement between our derived distances to nearby groups and those obtained from other distance estimators (Paper I) implies that diameter errors in the calibrating galaxies are not significant.

b) Sample Bias—The Malmquist Effect

Roberts (1978) has stressed that application of the Tully-Fisher technique to a magnitude-limited sample of *field galaxies* introduces a Malmquist bias into any determination of the Hubble constant. The present sample is drawn from a cluster (or supercluster) population which (the ambiguities discussed in § V aside) is all at the same distance, so we do not expect the Malmquist effect to be relevant. Two of the clusters in this paper, Pegasus I and Z74-23, are, in fact, sampled as deep in both magnitude *and* velocity width as Virgo. The latter is illustrated in Figure 7, which displays a velocity-width histogram of all galaxies in the current series (zero-weight objects excluded). Figure 7 shows that the Cancer cluster is sampled about two-thirds as deep as Virgo. Only the Perseus supercluster is sampled predominantly at the bright end.

We can derive a semiquantitative estimate of the importance of Malmquist bias. In the Tully-Fisher method the effect will manifest itself as a correlation between redshift and velocity width (Roberts 1978). These quantities for the present sample are plotted against each other in Figure 8, which the reader should compare to Figure 5 of Roberts (1978). The correlation coefficients between log ΔV and log V_0 are given in Table 11. No significant correlation is apparent.

If the H I content of cluster galaxies is reduced, then an observational bias will result in that highly inclined, low-H I galaxies will not be detected because of the low peak signal. However, there is no evidence that the H I content of our sample galaxies is low (see below), nor does the inclination correlate with either distance

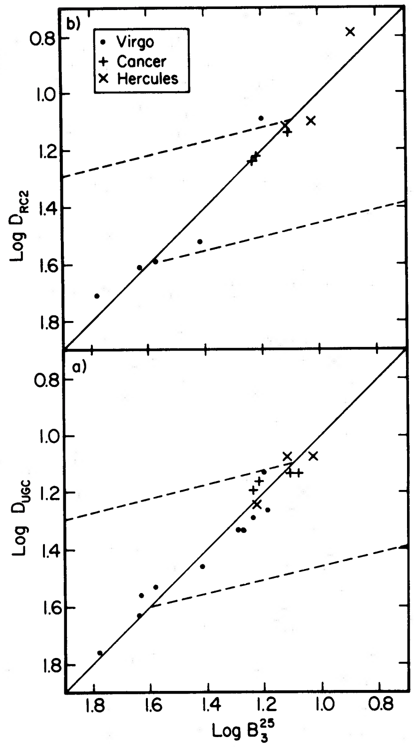

FIG. 6.—(*a*) UGC diameters transformed to the RC2 system vs. diameters in the B_3 system (see text) corresponding to an isophote of 25th mag arcsec^{-2}. (*b*) Diameters taken directly from the RC2 vs. B_3 diameters. In both cases the solid lines have slope unity, units are in 0.'1, and the dashed lines have the same significance as in Fig. 5.

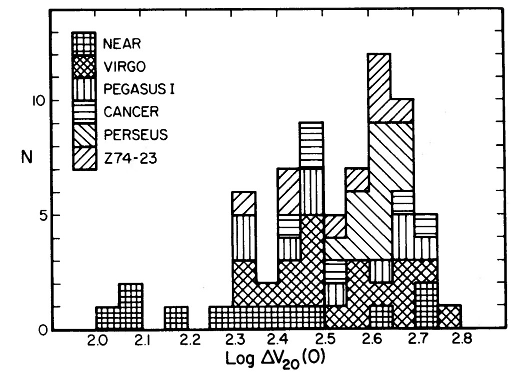

FIG. 7.—A velocity width histogram for (nonzero weighted) galaxies in Papers I and II and this paper. Note that two of the more distant clusters (Pegasus I and Z74-23) are sampled in velocity width to as deep a level as Virgo.

moduli or velocity width as would be expected if this bias were present.

Finally, we note that within the errors the distance moduli here do not depend on morphological type; a similar lack of dependence was found for the larger Virgo sample in Paper II. In that paper we also saw no dependence on the limiting magnitude either optically or at 21 cm, and so it seems unlikely that such bias occurs in the present sample.

c) *Environmental Effects*

Since the work of Oemler (1974), there has been little doubt that certain properties of galaxies in clusters are dependent on the nature of the cluster in which the galaxy finds itself. Some workers still strongly argue, however, that these properties are determined not by the cluster environment but by local conditions at the time of galaxy formation (Dressler 1980; Sandage and Visvanathan 1978*b*). For the present purposes, we concentrate on those particular properties of galaxies which determine their location in the Tully-Fisher diagram (see AHM and Mould 1979).

First, could the total mass-to-light ratios of galaxies in clusters vary systematically from cluster to cluster? Such changes would be incorrectly interpreted as differences in relative distance moduli. A number of mechanisms can be devised which lead to systematic variation in M/L within and outside clusters. For example, the apparently lower hydrogen-mass–to–luminosity ratio M_H/L for galaxies in Coma and Abell 1367 than for the field (Sullivan and Johnson 1978; Sullivan *et al.* 1980) might imply different star-formation rates leading to differing M/L values in these clusters. Star-formation rates could also be influenced by different rates of infall from the intra-cluster and intergalactic medium (Tinsley and Larson 1980). A differing quantity and/or distribution of "dark matter" inside and outside clusters might directly affect M/L. All of these mechanisms, however, are confronted by the closely similar Hubble ratios we obtain for the Perseus supercluster and the other distant clusters. The Perseus supercluster galaxies are almost all in an environment similar to the nearby calibrating galaxies. The supercluster results, therefore, argue both for the applicability of the absolute calibration of Paper I and for the lack of systematic

TABLE 11

SOLUTIONS TO LOG $\Delta V_{20}{}^c(0) = a + b(\text{LOG } V_0)$

Sample	N	*a*	*b*	*r*
Pegasus I..........	10	2.05	0.13	0.08
Cancer.............	6	4.02	-0.40	-0.33
Zwicky 74-23.......	9	3.62	-0.29	-0.20
Perseus Supercluster.....	13	2.01	0.16	0.20
Total..............	38	2.16	0.11	0.10

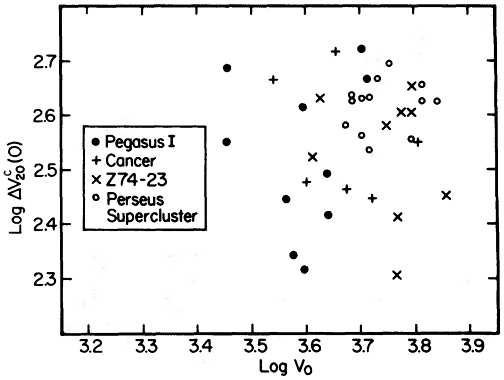

FIG. 8.—Corrected velocity widths from Table 6 plotted against corrected velocities from Tables 2 and 5. If the samples were biased because of Malmquist effect, a significant correlation between the two quantities would occur. No such correlation is seen (see text for further details).

M/L effect over the range of cluster types studied here. The latter conclusion is also supported by the normal $M_{\rm H}/L$ ratios found by Sullivan and collaborators in Pegasus, Cancer, and Z74-23.

Second, we should consider whether there are differences in internal dynamics between galaxies in clusters and those in the field. Note that the neutral hydrogen in the Tully-Fisher relation plays the role of a test medium for the potential field of the galaxy, so that simple reduction of the H I content in cluster galaxies should not affect the 21 cm line width. To product incorrect distances, we require either a drastic modification of the potential or a truncation of the gaseous disk before the rotation curve has reached the maximum or asymptotic velocity. Small systematic reductions in outer optical radii have been observed by Strom and Strom (1978) for ellipticals in spiral-poor clusters. But there is no evidence for systematic effects of the size required here. We would not expect such strong tidal interactions, since the encounter times in clusters are generally short because of the high relative velocities of the participant galaxies (e.g., Wright 1972).

Again, the strongest evidence we have that cluster density differences do not determine the internal dynamics of spirals is the agreement between the Perseus supercluster results and those for other denser clusters. An additional argument against density effects is provided by the close agreement in slope of the IR/H I relationship between Virgo ($b = 10.2$), the richest cluster in the sample, and the NGC 2403–M81 group ($b = 10.0$), the sparsest "cluster," since we might expect any dynamical changes to alter the fourth-power velocity-width dependence.

Clearly, the hypotheses discussed above can be further tested by observing more clusters of different densities and concentrations. For now, we consider the empirical answer to be the best and most immediately available. Until evidence to the contrary appears, we view the history and environment of a cluster as not being significant in determining its locus in the Tully-Fisher diagram.

VIII. IS SUCH A LARGE PERTURBATION TENABLE?

A crucial new result contained in this paper is the perturbation in the Hubble flow owing to the Local Supercluster. If this effect is real, any value of the Hubble constant deduced from the distance of the Virgo cluster, whether based on the Tully-Fisher relation, the diameters of H II regions, or whatever, must be increased by 45%. The size of the perturbation is, therefore, the critical question. In this section we discuss whether our results can reasonably be maintained in the face of a body of apparently conflicting evidence.

a) The Hubble Diagram for Giant Ellipticals

If giant elliptical galaxies are standard candles, the location of the Virgo galaxy NGC 4472 near the ridge line of the Hubble diagram (Sandage and Tammann 1976*b*) suggests that Virgo is rather close to its cosmological distance. With our value of H_0 (§ VI), NGC 4472 is overluminous relative to distant gE galaxies. How significant is this discrepancy?

The equation for the regression line of the simplest Hubble diagram for giant ellipticals (without B-M class or richness corrections) is given by Sandage (1972) as

$$V_c = 5 \log V_0 - 6.76 . \qquad (12)$$

In order to check the expected magnitude of NGC 4472, we must place Virgo at its cosmological redshift (1499 km s^{-1}), i.e., at a velocity corresponding to its distance and the assumed value of H_0. We must also adjust the magnitude to the correct metric diameter, since Sandage's (1972) measurements are within a circle of fixed linear size. This diameter is 86 kpc for $H_0 = 50$ km s^{-1} Mpc^{-1}, but 45 kpc for $H_0 = 95$ km s^{-1} Mpc^{-1}. At a Virgo distance of 15.6 Mpc (§ VI), the corresponding angular diameter is 9$'$.9. Two estimates of the NGC 4472 V magnitude in this size aperture can be made. First, extrapolation of de Vaucouleurs's (1961) 1$'$.8 measurement of 9.62 mag, using the mean growth curve given by Sandage (1975), yields $V = 8.65$ mag. Second, extrapolation of Holmberg's (1958) 11$'$ photographic magnitude of 8.49, again using Sandage's growth curve, gives $V = 8.54$ mag. The agreement is not entirely satisfactory. We adopt $V = 8.59$ mag, but a proper measurement of NGC 4472 in a 9$'$.9 aperture is feasible and should be made. Note that the value adopted by Sandage (1972) is $V = 8.45$ mag.

The magnitude predicted by equation (12) is 9.12. If we adopt a dispersion of 0.3 mag in the magnitudes of first-ranked cluster galaxies, the discrepancy of 0.54 mag makes NGC 4472 about 1.8 σ brighter than the mean. The uncertainty in the estimated discrepancy is $\sim$0.2 mag, composed of the error in the Virgo distance, the error in our adopted value of H_0 and the uncertainty in the NGC 4472 magnitude. Nine of the 84 galaxies in Sandage's (1972) Table 5 deviate further than NGC 4472; five of these would be intrinsically brighter than NGC 4472 on the present distance scale.

A larger formal discrepancy (2.2 σ) is derived for NGC 4472 if we use a more sophisticated Hubble diagram, such as that of Sandage, Kristian, and Westphal (1976), which has the latest corrections for B-M class and cluster richness. However, the additional uncertainty of the corrections in any particular case should be offset against this increased discrepancy. For example, a change of 1 in the B-M class for Virgo could reduce the discrepancy from 0.67 to 0.43 mag. Furthermore, because the B-M and richness correction are not derived in a redshift-independent manner, whether such corrections should be applied at all is a matter of some debate (Gunn 1978). No such corrections are adopted by Gunn and Oke (1975) in their analysis of the Hubble diagram.

In conclusion we feel that there is nothing strongly anti-Copernican in the absolute magnitude of NGC 4472 implied by our relative moduli for Virgo and the more distant clusters.

b) *Supernovae*

Comparison of the relative distance moduli of the Virgo and Coma clusters with the ratio of their redshifts is a good test of the perturbation in the observed Hubble flow proposed here. The best currently available Coma redshift is 6952 ± 61 km s^{-1} (Tifft and Gregory 1976), which is based on 226 galaxies within the 3° core. In Paper II we derived a new Virgo redshift of 1019 ± 51 km s^{-1}. The magnitude change between Virgo and Coma predicted by the ratio of redshifts is thus 4.17 ± 0.08 mag. This result should be, to first order, independent of any statistical correction for foreground or background objects, since the sample size and analysis for Virgo and Coma are comparable. Our predicted distance to Coma is $(7419 \pm 97)/(95 \pm 5) = 78.1 \pm 4.2$ Mpc, where the Coma redshift has now been adjusted for a 480 ± 75 km s^{-1} Local Group motion toward Virgo. Our Virgo distance of 15.6 ± 0.7 Mpc then leads to a predicted relative magnitude change of 3.50 ± 0.11 mag.

The supernovae test was applied by Tammann (1978), who used the relative apparent magnitudes of Type I supernovae in E/S0 galaxies in the Virgo and Coma clusters to put an upper limit on the peculiar motion of the Sun toward the Virgo cluster of 111 ± 140 km s^{-1}. More recently, Tammann, Sandage, and Yahil (1980) have argued that the agreement of this relative modulus (3.89 ± 0.21) with the mean of other methods discussed below establishes an infall velocity of the Local Group of 174 ± 74 km s^{-1}. The disagreement of Tammann's (1978) relative modulus from supernovae with the relative modulus of 3.50 ± 0.11 mag calculated above is a formal discrepancy of 1.6 σ. Overall discrepancy with our results persists, however, only if we are prepared to accept Tammann's (1978) argument that results from Type I supernovae in field spiral galaxies should be *ignored* because of Malmquist bias.

Like Tammann, we use the compilation of well-observed supernovae by Branch and Bettis (1978) in order to apply the supernovae test to field spirals. We also recorrect the apparent photographic magnitudes to the reddening model of Sandage and Visvanathan (1978*a*). If we suppose (as is elaborated in the next section) that the expansion rate within the Local Supercluster is on average 65 km s^{-1} Mpc^{-1}, but outside the Supercluster a value of 95 km s^{-1} Mpc^{-1} pertains, our results can be tested by comparing the calculated absolute magnitudes of Type I supernovae in spirals inside and outside the Supercluster.

The interior sample is conservatively defined by $V_0 < 1500$ km s^{-1}, the exterior sample by $V_0 > 2500$ km s^{-1}. With the above values of the expansion rate and no correction for internal absorption, $\langle M_{pg} \rangle = -18.9 \pm 0.18$ for the exterior sample ($\sigma = 0.50$, $n = 8$). Formal correction for Malmquist bias ($1.38\,\sigma^2$) reduces the latter value to $\langle M_{pg} \rangle = -18.5$, *coinciding with the interior sample* ($\langle M_{pg} \rangle = -18.5$, $\sigma = 0.68$, $n = 16$). The formal correction, however, is probably excessive, since it is by no means clear that all the scatter in Type I supernovae in spirals is intrinsic. Observational error and gravitational perturbation of the Hubble flow (clustering) may well contribute substantially.

A final, statistically weaker, but direct and unbiased test of our results is provided by the two supernovae observed in the Pegasus I cluster (SN 1970j in NGC 7619 and 1972j in NGC 7634). The relative distance modulus of Pegasus I and Virgo derived from these supernovae is 2.20 ± 0.36 mag, in agreement with our result of 2.35 ± 0.20 mag and contrary to the redshift ratio value of 2.96 ± 0.08 mag at the 2 σ level. We conclude that relative distance moduli obtained from supernovae are, within the uncertainties, consistent with the present findings.

c) *Color Magnitude Diagram for E and* S0 *Galaxies*

A further difficulty with the distance moduli derived here relative to the Virgo cluster is the conflict with the color-magnitude results of Visvanathan and Sandage (1977). Direct comparison can at present be made for only one cluster, Pegasus I, for which Visvanathan and Sandage obtain a distance modulus relative to Virgo of 2.75 ± 0.50 mag for four galaxies. However, there is a stronger conflict between their results for Coma, for which a much larger sample is available. They find $\Delta m = 3.89 \pm 0.20$ mag, compared with our predicted value of 3.50 ± 0.11 mag.

We have reexamined these results by using the *fully corrected ubV* photometry of Sandage and Visvanathan (1978*b*). Regression of 50 points for Virgo (by alternately considering $u - V$ and V_{26} as the independent variable and taking the mean and assigning half-weight to values with a colon) in their notation leads to

$$V_{26} = -8.762[(\mu - V)_{0.5}{}^{\mathrm{KE}} - 2.3] + 10.406 . \quad (13)$$

We have excluded the M100 Virgo dwarfs from this solution, because (*a*) their colors and magnitudes are more uncertain, (*b*) only *UBV* colors are available, which must be transformed to the *ubV* system, and (*c*) most significantly, they are bluer than any other galaxies in all the cluster samples and yet heavily weight the regressions. (Note that if we follow Sandage and Visvanathan 1978*b* in discarding nine additional galaxies and equally weighting the remaining, a virtually identical solution is obtained.) Application of equation (13) to the four Pegasus I galaxies results in $\Delta m = 2.43 \pm 0.26$ mag, in good agreement with our measured value of 2.35 ± 0.20 mag, but $2\,\sigma$ from the predicted redshift ratio of 2.96 ± 0.08 mag. For 15 Coma galaxies, we find $\Delta m = 3.72 \pm 0.15$ mag only, $1.2\,\sigma$ from our predicted value of 3.50 ± 0.11 mag but $2.6\,\sigma$ from the redshift ratio value of 4.17 ± 0.08 mag.

Aaronson (1980) has applied the color-magnitude test for Coma, using $u - K$ rather than $u - V$ colors, which has the advantage of doubling the sensitivity of the method. Thirty-one Virgo galaxies are available for defining the $u - K$, V_{26} calibration. When this calibration is applied to 13 Coma galaxies, the result is $\Delta m = 3.10 \pm 0.18$ mag. By considering a $K_{-0.3}$ magnitude rather than V_{26}, a procedure which involves less extrapolation of data, the test can then be applied to a total of 22 Coma galaxies. The result found by Aaronson (1980) is then $\Delta m = 2.90 \pm 0.16$ mag. The reason for the $\sim 3\,\sigma$ disagreement between these numbers and that obtained using *ubV* colors is presently unclear, but we note that the infrared colors lead to a difference substantially less than our predicted shift of 3.50 mag.

Finally, we consider Fornax, the only other cluster for which Visvanathan and Sandage (1977) have data for more than four members. The mean cluster redshift of $1527 \pm 100\ \mathrm{km\ s^{-1}}$ (Visvanathan and Sandage 1977) leads to a predicted relative distance modulus of 0.88 ± 0.13 mag from Virgo. This result becomes -0.49 ± 0.17 mag if the redshifts are corrected for a Local Group motion of $480 \pm 75\ \mathrm{km\ s^{-1}}$ toward Virgo. However, since Fornax is itself a probable member of the Local Supercluster, this latter value should be considered a *lower limit* if the retardation picture discussed in § IX is correct. Application of equation (13) to 15 Fornax galaxies in Visvanathan and Sandage (1977) gives $\Delta m = 0.16 \pm 0.17$ mag, a result that is again significantly less than that predicted by the redshift ratio.

To summarize, we believe that contrary to the conclusions of Visvanathan and Sandage (1977) the color-magnitude test provides considerable support for substantial Local Group motion toward Virgo.

d) *N Brightest Galaxies Test*

Relative distance moduli between clusters have been estimated by comparing magnitudes of the first N brightest galaxies. The most extensive recent study is by Weedman (1976), who obtained nuclear magnitudes for the 10 brightest galaxies in nine clusters and argued that there was no evidence for significant nonuniform Hubble flow. On the other hand, Rubin (1976) has reexamined Weedman's results and concluded that they in fact support the anisotropy measured by Rubin *et al.* (1976). For the present discussion, it is of interest to examine the various predictions of the relative Virgo-Coma distance modulus. Weedman (1976) finds that $\Delta m = 4.22 \pm 0.3$ mag. However, if the results in this paper are correct, then Weedman's metric diameter must be adjusted accordingly, leading to a lower value of $\Delta m = 4.05 \pm 0.3$ mag. Total magnitudes for seven of the 10 brightest Coma galaxies are available from the RC2 and yield $\Delta m = 3.70 \pm 0.42$. Note that total magnitudes are ~ 1.7 times as sensitive to distance changes as nuclear magnitudes (Weedman 1976). Finally, comparison of the first-ranked galaxies, NGC 4472 in Virgo and NGC 4889 in Coma, leads to $\Delta m = 3.06$ (Sandage 1972; RC2), which becomes $\Delta m = 3.44$ on applying the B-M and richness corrections of Sandage, Kristian, and Westphal (1976). In their entirety, the various results seem not incompatible with our predicted Virgo-Coma modulus of 3.50 ± 0.11 mag.

e) *Surface Brightnesses of Elliptical Galaxies*

Kormendy (1977) has used the correlation between effective radius r_e and apparent magnitude B_e within r_e to test for relative Virgo cluster motion. His sample contains 11 Virgo ellipticals and eight "field" galaxies (six E, two S0), and he finds no evidence for velocity perturbation of the field sample relative to Virgo. However, we note that seven of the eight galaxies have redshifts $< 2600\ \mathrm{km\ s^{-1}}$, and so they are probable Local Supercluster members. If the model discussed in § IX is correct, these galaxies will be perturbed by Virgo, and one might not expect a differing Hubble ratio to be detectable. The furthest object in Kormendy's sample is NGC 7619, which is in the Pegasus I cluster. If we correct Kormendy's (1977) $\log r_e$ value for NGC 7619 to the cluster distance in Table 7 here, it still lies well within the scatter of the data in his Figure 2.

Of more significance is recent work by Kormendy (1979) that gives (B_e, r_e) relations for galaxies in more distant clusters (including Perseus and Coma). Although the scatter is large, preliminary results indicate shifts in the (B_e, r_e) relations relative to Virgo that are consistent with the findings obtained in this paper.

f) *Other Anisotropy Tests*

Our results strongly contradict the identity of H_0 found by Sandage and Tammann (1975*a*, *b*) for nearby

$V \lesssim 2000$ km s^{-1} and distant $V \lesssim 6000$ km s^{-1} Sc I samples. At present, we can see no satisfactory resolution to this conflict, although we note that the revised absolute magnitude–luminosity class relation discussed in Paper II yields a value of $H_0 = 76$ km s^{-1} Mpc^{-1} when applied to Sandage and Tammann's (1975*b*) distant Sc I sample. Furthermore, aside from the difficulties of recognizing Sc I's at large redshifts, the original estimate of $\sigma \approx 0.4$ mag (Sandage and Tammann 1974) for the Sc I luminosity dispersion appears to have been too optimistic. A more recent analysis by Tammann, Yahil, and Sandage (1979) yields a value of $\sigma = 0.63$ mag.

In another analysis of spiral galaxies by de Vaucouleurs and Bollinger (1979), a variation in Hubble ratio with supergalactic latitude of $\Delta H = 25$ km s^{-1} Mpc^{-1} is detected. These authors do not interpret their results as a simple motion toward Virgo, but invoke a complicated rotating and expanding Local Supercluster model. Nevertheless, their value for the expansion rate outside the Local Supercluster agrees well with that obtained in this paper.

Peebles (1976) has analyzed the velocity field around Virgo with a linearized gravitational perturbation model. By using Sandage and Tammann's (1975*a*) distances and redshifts, Peebles finds a Local Group motion toward Virgo of 294 ± 83 km s^{-1}. Schechter's (1977) analysis of nearby bright spirals also provides support for some motion toward Virgo. He deduces a velocity toward the north galactic cap (and thus Virgo) of 239 ± 73 km s^{-1} from a sample of galaxies with $11 < m_B < 11.75$.

The best-known claim for detection of a peculiar motion of the Local Group is that of Rubin *et al.* (1976). Relative to a sample of 96 Sc I–Sc II galaxies (assumed to be standard candles) with $3500 < V_0 < 6500$ km s^{-1}, a motion of 454 ± 125 km s^{-1} was found, which after correction for solar motion yields a velocity of some 600 km s^{-1} in a direction almost perpendicular to the Virgo cluster. The uncertainties in this result have been rediscussed by Schechter (1977). In any event, there is a formal discrepancy between the Virgo component of the Rubin-Ford effect and the present results of more than 3 σ. A key observational weakness in the Rubin *et al.* (1976) analysis, however, is that the peculiar motion is detected as a reflection in a reference frame at ~ 5000 km s^{-1} (i.e., a 10% effect). In the present paper motion of the Local Group is detected as a discrepancy between the observed and cosmological redshift of Virgo—a 45% effect.

The latter method is also employed by Tammann, Yahil, and Sandage (1979). From a study of the luminosity function in the *Revised Shapley-Ames Catalog* (Sandage and Tammann 1979, hereafter RSA), these authors find a peculiar velocity of the Virgo cluster relative to the remaining RSA of 60 ± 132 km s^{-1}. Adoption of a Virgo redshift equal to 950 ± 60 km s^{-1} by Tammann, Sandage, and Yahil (1980)[9] increases this value to 174 ± 74 km s^{-1}.

However, a major weakness of this technique is that the reference frame of the RSA catalog lies, for the most part, within the Local Supercluster, leading to dilution of the measured effect. This test is thus a good one for peculiar motions within a small comoving volume, but a poor test for a change in the expansion rate from inside to outside the Local Supercluster.

g) 3 K *Microwave Background Experiments*

Two independent experiments by Corey and Wilkinson (1976) and by Smoot, Gorenstein, and Muller (1977) lead to similar detections of significant dipole anisotropy in the 3 K microwave-background radiation. Both experiments have since been repeated, and the effect now seems very well established (Smoot 1980; Smoot and Lubin 1979; Cheng *et al.* 1979). By taking a weighted average of all available measurements, White (1980) obtains a peculiar solar velocity of 360 ± 40 km s^{-1} toward $\alpha = 11^h.7 \pm 0^h.4$ and $\delta = +15° \pm 6°$ (1950). A 300 km s^{-1} solar motion correction then leads to a Local Group velocity of 540 $\pm$ 50 km s^{-1} toward $\alpha = 10^h.8$ and $\delta = -14°.0$, $\sim 35°$ from the direction of the Virgo cluster. The component of motion toward Virgo is thus 440 ± 50 km s^{-1}, in good agreement with our own estimate of 480 $\pm$ 75 km s^{-1}. This result is particularly noteworthy in that these are the only two claims for detection of anisotropy at a level greater than $\sim 5\,\sigma$.

h) *Conclusion*

The most conservative conclusion one should draw from this review is that there is no overriding evidence against the large perturbation in the Local velocity field detected here. Indeed, much of the available evidence supports our results. There are numerous lines of attack on the relative moduli of clusters, and further work to improve their quality will be helpful.

IX. COSMOLOGICAL IMPLICATIONS

To summarize, our preliminary results indicate a value of the expansion rate equal to 95 ± 5 km s^{-1} Mpc^{-1} and a Local Group motion of 480 $\pm$ 75 km s^{-1} toward Virgo. In this final section some further implications of our findings are discussed.

If we accept the idea of a Local Group motion toward Virgo, the next most important question is: How large is the comoving volume? The best answer that we can make at the moment is suggested by the absence of large shearing motions in the galactic neighborhood (Tammann and Kraan 1978; Sandage and Tammann 1975*a*). This implies that the low value of the expansion rate seen for the Virgo cluster is close to the general or mean expansion rate elsewhere within the Local Supercluster. Our results (AHM) for the Ursa Major cluster ($H = 61 \pm 4$ km s^{-1} Mpc^{-1} with the revised calibration of Paper I) and observations in

[9] The 69 km s^{-1} disagreement between Tammann, Sandage, and Yahil's Virgo redshift and that found in Paper II (1019 km s^{-1}) is almost entirely due to differing solar-motion corrections.

progress for NGC 2841, Leo, and other nearby groups support this generalization. This leads us to propose a deceleration model in which the expansion rate within the Supercluster is retarded by gravitational effects. Only beyond the Supercluster do we find the full expansion rate of the true Hubble flow. In a frame comoving with this unperturbed flow, an infall velocity toward Virgo is expected throughout the Supercluster. As a preliminary representation of the present results and the microwave-background anisotropy, we define a model with an expansion rate of 65 km s^{-1} Mpc^{-1} within the Local Supercluster and 95 km s^{-1} Mpc^{-1} outside. This is, of course, a zeroth order delineating of a dynamically plausible model, which must involve a radial gradient in the expansion rate for any reasonable mass distribution (cf. Peebles 1976). If we suppose the perturbation originates in a spherically symmetric system with a mean density contrast of 1.5–3.0, a range appropriate to the Local Supercluster (Gunn 1978), then Figure 1 of Silk (1974) leads to a density parameter

$$\Omega \sim 0.7\text{–}0.2\,. \tag{14}$$

In a simple expanding Friedmann universe, we then have for the deceleration parameter

$$q_0 \sim 0.35\text{–}0.1\,. \tag{15}$$

More realistic flattened models for the Local Supercluster, such as those of White and Silk (1979), can also account for the component of motion perpendicular to the supergalactic plane observed in the microwave background experiments.

The mass density range in equation (14) is reasonably consistent with other "local" tests of this parameter: Gunn's (1978) application of the "$L \times M/L$" method gives $\Omega \sim 0.1 \pm 0.1$. A similar value is obtained from Gunn's discussion of the deuterium abundance. Davis, Geller, and Huchra (1978) find $\Omega \sim 0.2$–0.7 by applying the statistical virial theorem to galaxies with $m_B < 13$. Finally, an analysis by Peebles (1979) of the Kirshner, Oemler, and Schechter (1978) galaxy sample leads to $\Omega \sim 0.4 \pm 0.2$.

Our results further imply an age of the universe given by $t_0 \lesssim 1 \times 10^{10}$ yr. This estimate appears in only marginal disagreement with the rather wide limits given by various elemental age tests (see Gunn 1978). A more serious conflict may exist with the ages of globular cluster stars— a classical problem in the quest for H_0. If our preliminary estimate of the Hubble expansion is borne out, we should perhaps look for some easing of this difficulty in the development of more satisfactory main-sequence models for the oldest stars.

We thank Graham Berriman for assistance at the telescope with some of these observations. We also thank Steve and Karen Strom for kindly providing full access to their plate material; Galen Gisler, John Kormendy, Nathan Krumm, Mort Roberts, Brent Tully, and Simon White for useful conversations; and Doug McElroy for his aid in preparing offsets. The generous allotment of telescope time at KPNO and Hale and Arecibo Observatories is greatfully acknowledged. One of us (M. A.) would especially like to thank G. Rieke, P. Strittmatter, R. Weymann, and R. Williams for their unconstrained financial support which enabled much of the work in this series of papers to be accomplished. We thank G. Neugebauer for the use of his infrared equipment at the Hale Observatories. This work was partially supported with funds from NSF grants AST 76-81874, AST 76-22991, AST 79-20516A1, and AST 79-21663; NASA grant NGL 05-002-207; and a grant from the University of Washington Graduate School Research Fund.

REFERENCES

Aaronson, M. 1980, in preparation.

Aaronson, M., Huchra, J., and Mould, J. 1979, *Ap. J.*, **229**, 1 (AHM).

Aaronson, M., Mould, J., and Huchra, J. 1980, *Ap. J.*, **237**, 000 (Paper I).

Bania, T. M., Thompson, L. A., and Thuan, T. X. 1980, in preparation.

Barbon, R. 1969, *Contr. Kitt Peak Nat. Obs.*, No. 510.

Barbon, R., and Capaccioli, M. 1974, *Astr. Ap.*, **35**, 151.

Branch, D., and Bettis, C. 1978, *A.J.*, **83**, 224.

Carney, B. 1979, private communication.

Cheng, E. S., Saulson, P. R., Wilkinson, D. T., and Corey, B. E. 1979, *Ap. J. (Letters)*, **232**, L139.

Chincarini, G., Giovanelli, R., and Haynes, M. P. 1980, *A.J.*, **84**, 1500.

Chincarini, G., and Rood, H. J. 1971, *Ap. J.*, **168**, 321.

———. 1972, *A.J.*, **77**, 4.

———. 1976, *Pub. A.S.P.*, **88**, 388.

Corey, B. E., and Wilkinson, D. T. 1976, *Bull. AAS*, **8**, 351.

Danver, C. G. 1942, *Ann. Obs. Lund.*, No. 10.

Davis, L., Latham, D., Huchra, J., and Tonry, J. 1979, private communication.

Davis, M., Geller, M. J., and Huchra, J. 1978, *Ap. J.*, **221**, 1.

de Vaucouleurs, G. 1961, *Ap. J. Suppl.*, **5**, 233.

———. 1978, *Ap. J.*, **223**, 730.

de Vaucouleurs, G., and Bollinger, G. 1979, *Ap. J.*, **233**, 433.

de Vaucouleurs, G., and de Vaucouleurs, A. 1967, *A.J.*, **72**, 730.

de Vaucouleurs, G., de Vaucouleurs, A., and Corwin, H. G. 1976, *Second Reference Catalogue of Bright Galaxies* (Austin: University of Texas Press) (RC2).

Disney, M. J., and Cromwell, R. H. 1971, *Ap. J. (Letters)*, **164**, L35.

Dressler, A. 1980, *Ap. J.*, **236**, 351.

Freeman, K. C. 1970, *Ap. J.*, **160**, 811.

Gregory, S., Thompson, L. A., and Tifft, W. G. 1980, in preparation.

Gunn, J. E. 1978, in *Observational Cosmology*, ed. A. Maeder, L. Martinet, and G. Tammann (Sauverny: Geneva Observatory), p. 1.

Gunn, J. E., and Oke, J. B. 1975, *Ap. J.*, **195**, 255.

Helou, G., Salpeter, E. E., and Krumm, N. 1979, *Ap. J. (Letters)*, **228**, L1.

Holmberg, E. 1958, *Medd. Lund Astr. Obs.*, Ser. 2, No. 136.

Humason, M. L., Mayall, N. U., and Sandage, A. R. 1956, *A.J.*, **61**, 97.

Jôeveer, M., Einasto, J., and Tago, E. 1978, *M.N.R.A.S.*, **185**, 357.

Kintner, E. C. 1971, *A.J.*, **76**, 409.
Kopylov, I. M., Lipovetsky, V. A., Pronik, V. I., and Chuvaev, K. K. 1974, *Astrofizika*. **10**, 483.
Kirshner, R. P., Oemler, A., and Schechter, P. L. 1978, *A.J.*, **83**, 1549.
Kormendy, J. 1977, *Ap. J.*, **218**, 333.
———. 1979, private communication.
Kowal, C. T., and Sargent, W. L. W. 1971, *A.J.*, **76**, 756.
Krumm, M., and Salpeter, E. E. 1979, private communication.
Mould, J. 1979, in *Photometry, Kinematics, and Dynamics of Galaxies*, ed. D. S. Evans (Austin: University of Texas Press).
Mould, J., Aaronson, M., and Huchra, J. 1980, *Ap. J.*, **238**, 458 (Paper II).
Nilson, P. N. 1973, *Uppsala General Catalogue of Galaxies*, *Uppsala Astr. Ann. Obs.*, Vol. **6** (UGC).
Oemler, A. 1974, *Ap. J.*, **194**, 1.
Peebles, P. J. E. 1976, *Ap. J.*, **205**, 318.
———. 1979, *A.J.*, **84**, 730.
Pence, W. 1976, *Ap. J.*, **203**, 39.
Peterson, B. M., Strom, S. E., and Strom, K. M. 1979, *A.J.*, **84**, 735.
Peterson, S. D., and Shostak, G. S. 1974, *A.J.*, **79**, 767.
Roberts, M. S. 1978, *A.J.*, **83**, 1026.
Rubin, V. C. 1976, in *IAU Colloquium 37, Decalages vers le rouge et expansion de l'univers* (Paris: C.N.R.S.), p. 119.
Rubin, V. C., Ford, W. K., Thonnard, N., Roberts, M. S., and Graham, J. A. 1976, *A.J.*, **81**, 687.
Sandage, A. 1961, *Ap. J.*, **133**, 355.
———. 1972, *Ap. J.*, **178**, 1.
———. 1973, *Ap. J.*, **183**, 711.
———. 1975, *Ap. J.*, **202**, 563.
———. 1978, *A.J.*, **83**, 904.
Sandage, A., and Hardy, E. 1973, *Ap. J.*, **183**, 743.
Sandage, A., Kristian, J., and Westphal, J. A. 1976, *Ap. J.*, **205**, 688.
Sandage, A., and Tammann, G. A. 1974, *Ap. J.*, **194**, 559.
———. 1975*a*, *Ap. J.*, **196**, 313.
———. 1975*b*, *Ap. J.*, **197**, 265.
———. 1976*a*, *Ap. J.* (*Letters*), **207**, L1.
———. 1976*b*, *Ap. J.*, **210**, 7.
———. 1979, *Revised Shapley-Ames Catalog* (Washington: Carnegie Institution of Washington), in press (RSA).
Sandage, A., and Visvanathan, N. 1978*a*, *Ap. J.*, **223**, 707.
———. 1978*b*, *Ap. J.*, **225**, 742.
Sargent, W. L. W. 1970, *Ap. J.*, **160**, 405.
Schechter, P. L. 1977, *A.J.*, **82**, 569.
Schommer, R. A., Sullivan, W. T., III, and Bothun, G. D. 1980, in preparation.
Schweizer, F. 1976, *Ap. J.*, *Suppl.*, **31**, 313.
Shostak, G. S. 1978, *Astr. Ap.*, **68**, 321.
Silk, J. 1974, *Ap. J.*, **193**, 525.
Smoot, G. F. 1980, *Phys. Scripta*, **21**, 619.
Smoot, G. F., Gorenstein, M. V., and Muller, R. A. 1977, *Phys. Rev. Letters*, **39**, 898.
Smoot, G. F., and Lubin, P. M. 1979, *Ap. J.* (*Letters*), **234**, L83.
Strom, K. M., and Strom, S. E. 1978, *A.J.*, **83**, 73.
Sullivan, W. T., III, and Johnson, P. E. 1978, *Ap. J.*, **225**, 751.
Sullivan, W. T., III, Schommer, R. A., Bothun, G. D., and Bates, B. A. 1980, in preparation.
Tammann, G. A. 1978, *Mem. Soc. Astr. Italy*, **49**, 315.
Tammann, G. A., and Kraan, R. 1978, in *IAU Symposium 79, Large Scale Structure of the Universe*, ed. M. S. Longair and J. Einasto (Dordrecht: Reidel), p. 71.
Tammann, G. A., Sandage, A., and Yahil, A. 1980, *Phys. Scripta*, **21**, 630.
Tammann, G. A., Yahil, A., and Sandage, A. 1979, *Ap. J.*, **234**, 775.
Thompson, L. A., Welker, W. J., and Gregory, S. A. 1978, *Pub. A.S.P.*, **90**, 644.
Tifft, W. G., and Gregory, S. A. 1976, *Ap. J.*, **205**, 696.
Tifft, W. G., Jewsbury, C. P., and Sargent, T. A. 1973, *Ap. J.*, **185**, 115.
Tinsley, B. M., and Larson, R. 1980, preprint.
Tully, R. B., and Fisher, J. R. 1977, *Astr. Ap.*, **54**, 661.
Turner, E. L. 1976, *Ap. J.*, **208**, 20.
Visvanathan, N., and Sandage, A. 1977, *Ap. J.*, **216**, 214.
Weedman, D. W. 1976, *Ap. J.*, **203**, 6.
White, S. D. M. 1980, *Phys. Scripta*, **21**, 640.
White, S. D. M., and Silk, J. 1979, *Ap. J.*, **231**, 1.
Wright, A. E. 1972, *M.N.R.A.S.*, **157**, 309.
Zel'dovich, Ya. B. 1978, in *IAU Symposium 79, Large Scale Structure of the Universe*, ed. M. S. Longair and J. Einasto (Dordrecht: Reidel), p. 409.
Zwicky, F., Herzog, E., Wild, P., Karpowicz, M., and Kowal, C. T. 1961–1968, *Catalogue of Galaxies and of Clusters of Galaxies*, 6 vols. (Pasadena: California Institute of Technology).

MARC AARONSON: Steward Observatory, University of Arizona, Tucson, AZ 85721

GREGORY D. BOTHUN and WOODRUFF T. SULLIVAN, III: Department of Astronomy, FM-20, University of Washington, Seattle, WA 98195

JOHN HUCHRA: Center for Astrophysics, 60 Garden Street, Cambridge, MA 02138

JEREMY MOULD: Kitt Peak National Observatory, P.O. Box 26732, Tucson, AZ 85726

ROBERT A. SCHOMMER: Yerkes Observatory, Williams Bay, WI 53191